CHEMISTRY
A EUROPEAN JOURNAL

DOI: 10.1002/chem.200600160

Acid–Base and Metal-Ion-Binding Properties of Xanthosine 5′-Monophosphate (XMP) in Aqueous Solution: Complex Stabilities, Isomeric Equilibria, and Extent of Macrochelation**

Helmut Sigel,*[a] Salah S. Massoud,[b] Bin Song,[a, c] Rolf Griesser,[a] Bernd Knobloch,[a, d] and Bert P. Operschall[a]

Dedicated to Professor Dr. Bernhard Lippert on the occasion of his 60th birthday, with admiration for his seminal contributions to the chemistry of nucleobases

Abstract: The four acidity constants of threefold protonated xanthosine 5′-monophosphate, $H_3(XMP)^+$, reveal that at the physiological pH of 7.5 $(XMP-H)^{3-}$ strongly dominates (and not XMP^{2-} as given in textbooks); this is in contrast to the related inosine (IMP^{2-}) and guanosine 5′-monophosphate (GMP^{2-}) and it means that XMP should better be named as xanthosinate 5′-monophosphate. In addition, evidence is provided for a tautomeric $(XMP-H{\cdot}N1)^{3-}/(XMP-H{\cdot}N3)^{3-}$ equilibrium. The stability constants of the $M(H;XMP)^+$ species were estimated and those of the M(XMP) and $M(XMP-H)^-$ complexes ($M^{2+}=Mg^{2+}$, Ca^{2+}, Sr^{2+}, Ba^{2+}, Mn^{2+}, Co^{2+}, Ni^{2+}, Cu^{2+}, Zn^{2+}, Cd^{2+}) measured potentiometrically in aqueous solution. The primary M^{2+} binding site in M(XMP) is (mostly) N7 of the monodeprotonated xanthine residue, the proton being at the phosphate group. The corresponding macrochelates involving $P(O)_2(OH)^-$ (most likely outer-sphere) are formed to ≈65% for nearly all M^{2+}. In $M(XMP-H)^-$ the primary M^{2+} binding site is (mostly) the phosphate group; here the formation degree of the N7 macrochelates varies widely from close to zero for the alkaline earth ions, to ≈50% for Mn^{2+}, and ≈90% or more for Co^{2+}, Ni^{2+}, Cu^{2+}, Zn^{2+}, and Cd^{2+}. Because for $(XMP-H)^{3-}$ the micro stability constants quantifying the M^{2+} affinity of the xanthosinate and PO_3^{2-} residues are known, one may apply a recently developed quantification method for the chelate effect to the corresponding macrochelates; this chelate effect is close to zero for the alkaline earth ions and it amounts to about one log unit for Co^{2+}, Ni^{2+}, Cu^{2+}. This method also allows calculation of the formation degrees of the monodentatally coordinated isomers; this information is of relevance for biological systems because it demonstrates how metal ions can switch from one site to another through macrochelate formation. These insights are meaningful for metal-ion-dependent reactions of XMP in metabolic pathways; previous mechanistic proposals based on XMP^{2-} need revision.

Keywords: alkaline earth metals · bioinorganic chemistry · chelates · isomers · nucleotides · transition metals · xanthosinate

[a] Prof. Dr. H. Sigel, Dr. B. Song, Dr. R. Griesser, Dr. B. Knobloch, Dipl. Ing. B. P. Operschall
Department of Chemistry, Inorganic Chemistry
University of Basel, Spitalstrasse 51, 4056 Basel (Switzerland)
Fax: (+41) 61-267-1017
E-mail: helmut.sigel@unibas.ch

[b] Prof. Dr. S. S. Massoud
Department of Chemistry
University of Louisiana at Lafayette
P. O. Box 44370, Lafayette, LA 70504-4370 (USA)

[c] Dr. B. Song
AnorMed Inc., #200, 20353-64 Avenue
Langley, BC, V2Y 1N5 (Canada)

[d] Dr. B. Knobloch
Institute of Inorganic Chemistry
University of Zürich, Winterthurerstrasse 190
8057 Zürich (Switzerland)

[**] Abbreviations and definitions (see also Figure 1): ATP^{4-}, adenosine 5′-triphosphate; Bz, benzimidazole-type ligand; Cyd, cytidine; GMP^{2-}, guanosine 5′-monophosphate (Figure 1); *I*, ionic strength; IMP^{2-}, inosine 5′-monophosphate (Figure 1); K_a, general acidity constant; M^{2+}, general divalent metal ion; 9MeXan, 9-methylxanthine; NMP^{2-}, nucleoside 5′-monophosphate; $R\text{-}PO_3^{2-}$, simple phosphate monoester or phosphonate ligand with R representing a noninteracting residue; Xan, xanthine; Xao, xanthosine; XMP^{2-}, xanthosine 5′-monophosphate (see Figure 1 and Figure 4 and their legends). Species written without a charge (e.g., XMP) either do not carry one or represent the species in general (i.e., independent of their protonation degree); which of the two possibilities applies is always clear from the context. In formulas such as $M(H;XMP)^+$, the H^+ ion and XMP^{2-} are separated by a semicolon to facilitate reading, yet they appear within the same parenthesis to indicate that the proton is at the ligand without defining its location. A formula like $(XMP-H)^{3-}$ means that the compound has lost a further proton and is to be read as XMP^{2-} *minus* H^+.

1. Introduction

Xanthosine 5′-monophosphate (XMP) is an important intermediate in the metabolism of nucleotides[1] and its production in dependence on the cellular energetic status was recently studied.[2] XMP is synthesized from inosine 5′-monophosphate (IMP^{2-}) and then it is converted with glutamine and adenosine 5′-triphosphate (ATP^{4-}) by GMP synthetase to guanosine 5′-monophosphate (GMP^{2-}; see Figure 1)[3–7]

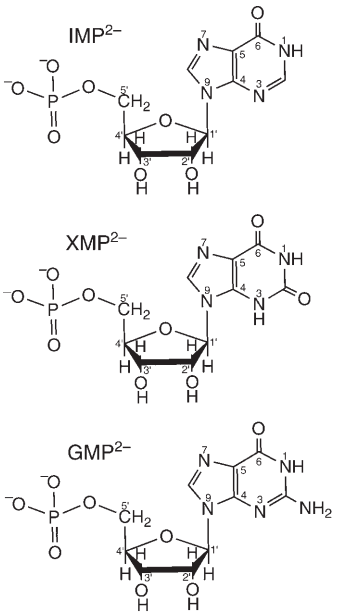

Figure 1. Chemical structure of xanthosine 5′-monophosphate (XMP^{2-}) in comparison with those of its relatives inosine 5′-monophosphate (IMP^{2-}) and guanosine 5′-monophosphate (GMP^{2-}). All these purine nucleotides are shown in their dominating *anti* conformation.[3–6] It is important to note that the structure shown above for *twofold* negatively charged XMP is the one commonly found in the literature including textbooks. Unfortunately this structure represents a *minority* species and is thus *misleading* regarding the distribution of the protons: The fact is[7] that the (N3)H/(N1)H sites have lost one proton (see also Figure 4 below), whereas the phosphate group still carries one. This means, one of the two negative charges is located in the pyrimidine ring and the other one at the phosphate group and it is this tautomer which occurs with the dominating formation degree of about 88%;[7] it is symbolized as $(X-H{\cdot}MP{\cdot}H)^{2-}$ and is discussed further in Section 2.2.

under release of glutamate and adenosine 5′-monophosphate (AMP^{2-}) and diphosphate.[1] This set of reactions certainly involves metal ions, especially in the step(s) employing ATP, which is virtually only a substrate in the form of its complexes.[8,9]

On the other hand, the degradation of AMP, IMP, GMP, and XMP to uric acid in humans also proceeds via xanthine, the purine nucleobase of XMP.[1] For example, following the cleavage of the *N*-glycosidic bond, guanine, the nucleobase of GMP, is converted in one step to xanthine by the heterolytic enzyme guanase.[10] Thereafter xanthine is transformed to uric acid by the molybdenum-containing enzyme xanthine oxidase,[1] a reaction which likely involves coordination of a $Mo^{IV/VI}$ unit to N7 of xanthine.[11]

Considering the central metabolic roles of XMP and the involvement of metal ions in these processes, it is surprising to find that the metal-ion-binding properties of this nucleotide have not been studied in a comprehensive way.[12–14] One of the reasons may be that the acid–base properties of XMP are relatively complicated (see legend to Figure 1).[7] However, the macro acidity constants of $H_3(XMP)^+$ have recently been obtained and some insights in the intrinsic acid–base properties of the (N1)H and (N3)H sites have been gained.[7] It was pointed out that the xanthine residue is deprotonated in the lower pH range, that is, below the physiological pH. This needs to be emphasized, because it means that a large part of the XMP structures shown in the literature, including textbooks, are incorrect. In fact, at the same time when our study[7] was published a review of Shugar et al.[15] appeared and these authors reached, based on various literature data, also the conclusion that at the physiological pH the xanthine residue is present in xanthosine and its nucleotides in the monodeprotonated form (see legend of Figure 1). Furthermore, they continue[15] "the foregoing has, somewhat surprisingly, been widely overlooked in studies on the properties of these compounds in various enzyme systems and metabolic pathways".[15]

In the course of our studies devoted to the coordination chemistry of nucleotides[8,16–20] we have now endeavored to resolve the indicated (N1)H versus (N3)H deprotonation ambiguity somewhat further and to determine the stability constants of several XMP–metal-ion complexes of varying protonation degrees. The complexes studied are those formed with the alkaline earth ions and with Mn^{2+}, Co^{2+}, Ni^{2+}, Cu^{2+}, Zn^{2+} or Cd^{2+}. It was the aim to quantify the equilibria between various isomeric species and to define the structures of these complexes in solution as far as possible. In addition, comparisons are made with the corresponding complexes involving IMP and GMP.[21] These insights ask for revision of previous mechanistic proposals.[22]

2. Results and Discussion

All experiments were carried out under conditions under which the self-association of XMP is expected to be negligible, due to previous experience with related nucleotides.[23,24] The potentiometric pH titrations for the determination of the stability constants of the complexes were made with solutions that were 0.3 mM in XMP and under these conditions with certainty[21] the monomeric forms are studied.

2.1 Definition and some comments on the acidity constants of $H_3(XMP)^+$: From the structure shown for XMP in Figure 1 it is evident that the phosphate group can accept two protons and, as known[21] from nucleotides like IMP and GMP, N7 can also be protonated. Furthermore, the (N1)H/(N3)H sites[7] and possibly also the ribose residue[25] can be deprotonated; hence, overall the following five deprotonation reactions [Eqs. (1)–(5)] need to be considered:

$$H_3(XMP)^+ \rightleftharpoons H_2(XMP)^{\pm} + H^+ \quad (1a)$$

$$K^H_{H_3(XMP)} = [H_2(XMP)^{\pm}][H^+]/[H_3(XMP)^+] \quad (1b)$$

$$H_2(XMP)^{\pm} \rightleftharpoons H(XMP)^- + H^+ \quad (2a)$$

$$K^H_{H_2(XMP)} = [H(XMP)^-][H^+]/[H_2(XMP)^{\pm}] \quad (2b)$$

$$H(XMP)^- \rightleftharpoons XMP^{2-} + H^+ \quad (3a)$$

$$K^H_{H(XMP)} = [XMP^{2-}][H^+]/[H(XMP)^-] \quad (3b)$$

$$XMP^{2-} \rightleftharpoons (XMP{-}H)^{3-} + H^+ \quad (4a)$$

$$K^H_{XMP} = [(XMP{-}H)^{3-}][H^+]/[XMP^{2-}] \quad (4b)$$

$$(XMP{-}H)^{3-} \rightleftharpoons (XMP{-}2H)^{4-} + H^+ \quad (5a)$$

$$K^H_{(XMP-H)} = [(XMP{-}2H)^{4-}][H^+]/[(XMP{-}H)^{3-}] \quad (5b)$$

The above equilibria define macro acidity constants, but in the way the species are written no information is provided about the locations of the protons. This information has recently been assembled[7] and is now shortly summarized:

In $H_3(XMP)^+$ two protons are at the phosphate group and one is at N7;[7] in a rough approximation one may say that the first proton [Eq. (1)] is released from the $P(O)(OH)_2$ group and the second one [Eq. (2)] from the $(N7)H^+$ site: The corresponding macro acidity constants are $pK^H_{H_3(XMP)} = 0.44 \pm 0.27$ and $pK^H_{H_2(XMP)} = 0.97 \pm 0.15$, respectively.[7] It is evident that the two equilibria involved are overlapping and that $H_2(XMP)$ exists in two tautomeric forms. It was estimated[7] that the zwitterionic species $(H{\cdot}XMP{\cdot}H)^{\pm}$, in which one proton is at the phosphate group and one at N7, dominates with about 70%, while $(XMP{\cdot}H_2)^0$ with both protons at the phosphate residue forms to about 30%. However, because both mentioned pK_a values are either below or close to 1, they are not of relevance for the present study which deals with the pH range above 3.2. The only value needed from the earlier evaluations[7] is the micro acidity constant of the zwitterionic $(H{\cdot}XMP{\cdot}H)^{\pm}$ tautomer, $pk^{XMP{\cdot}H}_{H{\cdot}XMP{\cdot}H} = 1.11 \pm 0.08$, which quantifies the intrinsic acidity of the $(N7)H^+$ unit in this species and which allows to estimate the stability of $M(H;XMP)^+$ complexes (see Section 2.6).[26]

In the $H(XMP)^-$ species the xanthosine residue is uncharged and the phosphate residue carries one proton. This species easily loses two protons[7] with the acidity constants $pK^H_{H(XMP)} = 5.30 \pm 0.02$ [Eq. (3)] and $pK^H_{XMP} = 6.45 \pm 0.02$ [Eq. (4)]; that is, one proton from the nucleobase residue and one from the monoprotonated phosphate group, respectively. Further deprotonation of $(XMP{-}H)^{3-}$ occurs only with $pK_a > 12.0$ [Eq. (5)].[7] This means, that after monodeprotonation of either (N1)H or (N3)H, the remaining (N)H can be deprotonated as well,[27] as can the ribose residue,[25] and thus, it is not certain which deprotonation reaction in Equilibrium (5) actually takes place; most likely first the ribose ring loses a proton,[25] followed by that from the remaining (N)H site ($pK_a \cong 13$).[28] In any case, under our experimental conditions with evaluations for complex formation at $pH \leq 8.2$ a deprotonation according to Equilibrium (5) with $pK_a > 12.0$ is of no relevance and also not of biological interest.

2.2 Solution structures of the $H(XMP)^-$, XMP^{2-}, and $(XMP{-}H)^{3-}$ species: From Section 2.1 it follows that for this study, which encompasses the pH range 3.2–8.2, Equilibria (3) and (4) with the mentioned acidity constants $pK^H_{H(XMP)} = 5.30 \pm 0.02$ [Eq. (3)] and $pK^H_{XMP} = 6.45 \pm 0.02$ [Eq. (4)] are of relevance as far as complex formation is concerned. In a first approximation[7] $pK^H_{H(XMP)}$ quantifies the release of the proton from the xanthine residue and pK^H_{XMP} the final deprotonation of $P(O)_2(OH)^-$. In other words, the deprotonation of $H(XMP)^-$, better written as $(XMP{\cdot}H)^-$ and quantified by $pK^H_{H(XMP)}$ [Eq. (3)], gives rise to the species $(X{-}H{\cdot}MP{\cdot}H)^{2-}$ in which the xanthine moiety is deprotonated and the phosphate group still carries a proton.

The above consideration leads then to the question: Does an XMP^{2-} species as written in Equilibrium (3) with a neutral xanthine residue and a twofold negatively charged phosphate group (see also Figure 1) exist at all? This question was recently answered by application of the micro acidity constant scheme shown in Figure 2. From the microconst-

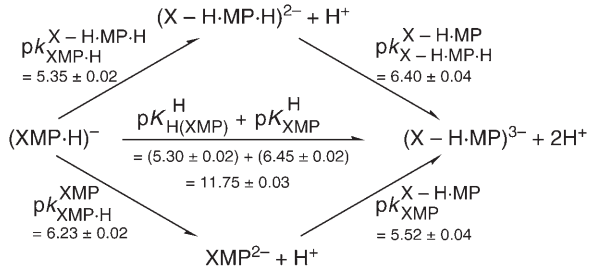

Figure 2. Equilibrium scheme for $(XMP{\cdot}H)^-$ to $(X{-}H{\cdot}MP)^{3-}$ defining the micro acidity constants (k) together with the measured macro acidity constants (K) and the interrelation between $(X{-}H{\cdot}MP{\cdot}H)^{2-}$ and XMP^{2-} and the other species present. In $(X{-}H{\cdot}MP{\cdot}H)^{2-}$ the xanthine residue is deprotonated and the proton located at the phosphate group; in its XMP^{2-} tautomer the nucleobase is uncharged and the phosphate group deprotonated. $(XMP{\cdot}H)^-$ and $(X{-}H{\cdot}MP)^{3-}$ are also often written as $H(XMP)^-$ [Eqs. (2), (3)] and $(XMP{-}H)^{3-}$ [Eq. (4)], respectively. The arrows indicate the direction for which the acidity constants are defined. For details see reference [7].

ants given there it follows that the answer to the question is "yes" and that the simple XMP^{2-} species occurs with a formation degree of about 12% in equilibrium with the dominating $(X{-}H{\cdot}MP{\cdot}H)^{2-}$ tautomer possessing a deprotonated xanthine residue and a monoprotonated phosphate group; its formation degree is about 88%.[7]

However, more important for the structural evaluation of the metal ion complexes to be considered below in Sections 2.7–2.10 is that the intrinsic acidity of the xanthine residue in $(XMP{\cdot}H)^-$ is quantified by the micro acidity con-

stant $pk^{X-H\cdot MP\cdot H}_{XMP\cdot H} = 5.35 \pm 0.02$ and the one of XMP^{2-} by $pk^{X-H\cdot MP}_{XMP} = 5.52 \pm 0.04$ (Figure 2). Similarly, the intrinsic acidity of the $P(O)_2(OH)^-$ group in $(X-H\cdot MP\cdot H)^{2-}$ is given by $pk^{X-H\cdot MP}_{X-H\cdot MP\cdot H} = 6.40 \pm 0.04$; this latter value may be compared with the macroconstant $pK^{H}_{XMP} = 6.45 \pm 0.02$.[7]

The question that remains to be answered is: Which (N)H site, (N1)H or (N3)H, is deprotonated in the species $(XMP\cdot H)^-$ and XMP^{2-}? Despite severe discrepancies in the literature there seems now to be kind of a general agreement that the (N3)H site is the more acidic one in 9-methylxanthine as well as in xanthosine and its nucleotides,[15,29,30] but indications have been summarized[7] that the (N1)H-deprotonated tautomer also occurs in aqueous solution as a minority species. The preference for (N3)H appears to be largely based on a crystal structure analysis[31] of the sodium salt of xanthine, which shows a deprotonated $(N3)^-$ site.

However, there is also an X-ray structure[32] of a titanocene–xanthine 3:1 complex, $[\{Ti^{III}(\eta^5\text{-}C_5H_5)_2\}_3Cl(Xan-2H)]$, in which xanthine is twofold deprotonated, that is, at its N1 and N9 sites, whereas the (N3)H site remains intact.

2.3 Evaluation of the (N1)H versus (N3)H deprotonation ambiguity: Our above indication[7] that in aqueous solution actually tautomeric equilibria between (N1)H/$(N3)^-$ and $(N1)^-$/(N3)H exist for $(Xao-H)^-$, XMP^{2-}, and $(XMP-H)^{3-}$ can be further assessed. The review by Shugar et al.[15] already mentioned in Section 1 contains acidity constants for xanthosine and also for 1-methylxanthosine. The values were collected by these authors from the literature and partly also reproduced and measured by spectrophotometry in their own laboratory. The pK_a for Xao given in this publication[15] differs somewhat from the one determined by us by means of potentiometric pH titrations;[7] we attribute this discrepancy to differences in ionic strength. To eliminate systematic errors we use for the following evaluation only data from Shugar et al.;[15] these three values are printed in *italics* in the micro acidity constant scheme seen in Figure 3.

There are two macro acidity constants given on the horizontal arrow in Figure 3; they refer to Xao. The pK_a value of 13 is not really meaningful for the reasons summarized in the last paragraph of Section 2.1 and therefore, is used here only to complete the scheme but it is *not* used for further evaluations.

Because the four micro acidity constants can be interlinked with the two macroconstants only by the three equations given in the lower part of Figure 3, one of the microconstants needs to be estimated, thereafter the others can be calculated. The value for the deprotonation of (N3)H of Xao, $pk^{Xao-H\cdot N3}_{Xao}$ (Figure 3, upper part, left), can be simulated by the pK_a value of 1-methylxanthosine. In this compound only (N3)H can be deprotonated and it is not expected that the replacement of a hydrogen atom at N1 by a methyl group alters the acid–base properties of the (N3)H site, because H and CH_3 have very similar electronegativities; in fact, it has been proven[33] for several nucleobase derivatives that such a substitution does not affect the acid–base properties of sites close by. Hence, the pK_a value of 1-methylxanthosine[15] is set equal to $pk^{Xao-H\cdot N3}_{Xao}$ and is given in *italics*; now, by application of Equations (a) through (c) given in Figure 3, the upper and lower pathways in the scheme can be completed.

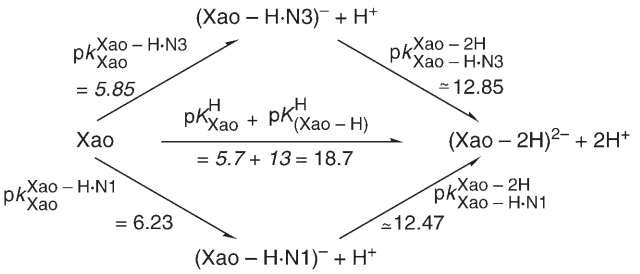

$$K^{H}_{Xao} = k^{Xao-H\cdot N3}_{Xao} + k^{Xao-H\cdot N1}_{Xao} \quad \text{(a)}$$

$$\frac{1}{K^{H}_{(Xao-H)}} = \frac{1}{k^{Xao-2H}_{Xao-H\cdot N3}} + \frac{1}{k^{Xao-2H}_{Xao-H\cdot N1}} \quad \text{(b)}$$

$$K^{H}_{Xao} \cdot K^{H}_{(Xao-H)} = k^{Xao-H\cdot N3}_{Xao} \cdot k^{Xao-2H}_{Xao-H\cdot N3} = k^{Xao-H\cdot N1}_{Xao} \cdot k^{Xao-2H}_{Xao-H\cdot N1} \quad \text{(c)}$$

Figure 3. Equilibrium scheme for Xao to $(Xao-2H)^{2-}$ defining the micro acidity constants (k) and showing their interrelation with the measured macro acidity constants (K) and the connection between $(Xao-H\cdot N3)^-$ and $(Xao-H\cdot N1)^-$ and the other species present. In $(Xao-H\cdot N3)^-$ the xanthine residue is deprotonated at the (N3)H site and in its $(Xao-H\cdot N1)^-$ tautomer the nucleobase is deprotonated at its (N1)H site. The arrows indicate the direction for which the acidity constants are defined. Use of the acidity constant measured[15] for the deprotonation of the (N3)H site in 1-methylxanthosine for the microconstant $pk^{Xao-H\cdot N3}_{Xao}$ (upper pathway at the left) permits calculation of the other microconstants with Equations (a), (b), and (c). The three values printed in *italics* are from reference [15]; the value of 13 for $pK^{H}_{(Xao-H)}$ contains some uncertainty. However, this uncertainty has no effect on the calculations given in Equation (7), which are based on the values given in the left part of the scheme. For details see text in Section 2.3.

The micro acidity constants of Figure 3 can now be applied to estimate for the tautomeric Equilibrium (6) the ratio R [Eq. (7)] of the monodeprotonated and isocharged species $(Xao-H\cdot N3)^-$ and $(Xao-H\cdot N1)^-$:

$$(Xao-H\cdot N1)^- \rightleftharpoons (Xao-H\cdot N3)^- \quad (6)$$

$$R_{(Xao-H)} = \frac{[(Xao-H\cdot N3)^-]}{[(Xao-H\cdot N1)^-]} = \frac{k^{Xao-H\cdot N3}_{Xao}}{k^{Xao-H\cdot N1}_{Xao}} \quad (7a)$$

$$= \frac{10^{-5.85}}{10^{-6.23}} = 10^{0.38} \quad (7b)$$

$$= \frac{2.40}{1} \quad (7c)$$

$$\approx \frac{70}{30}\left(\frac{63}{37};\frac{77}{23}\right) \quad (7d)$$

The ratio in Equation (7d) corresponds to the approximate percentages of the $(Xao-H\cdot N3)^-$ and $(Xao-H\cdot N1)^-$

species. The error limits given in parentheses of Equation (7d) are based on the information provided by Shugar et al.[15] that for their pK_a values ± 0.1 holds; hence, we attributed to $10^{0.38}$ in Equation (7b) an error of 0.14, that is, $10^{(0.38\pm0.14)}$. Thus, from $10^{0.24}$ follows the ratio 63/37 and $10^{0.52}$ gives 77/23. Hence, we may conclude that the N3-deprotonated species, $(Xao-H{\cdot}N3)^-$, dominates with about 70%, while the N1-deprotonated tautomer, $(Xao-H{\cdot}N1)^-$, forms to about 30%. Certainly, this result is only an estimation and therefore, it would be highly desirable that the various methylated derivatives of Xao and XMP are synthesized and their pK_a values measured. However, the present result still proves that both tautomeric forms of $(Xao-H)^-$ occur simultaneously in appreciable amounts and this may safely also be concluded for the $XMP^{2-}=(X-H{\cdot}MP{\cdot}H)^{2-}$ and $(XMP-H)^{3-}=(X-H{\cdot}MP)^{3-}$ species. Because the last mentioned compound is formed with $pK^{H}_{XMP}=6.45$ (or more exact $pk^{X-H{\cdot}MP}_{X-H{\cdot}MP{\cdot}H}=6.40\pm0.04$; Figure 2), the dominating species at the physiological pH of about 7.5 is $(X-H{\cdot}MP)^{3-}$, that is, xanthosinate 5′-monophosphate; it is this species which is shown in Figure 4 and which should be depicted in

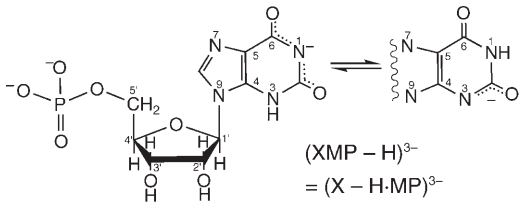

Figure 4. Chemical formula of the structure of XMP at the physiological pH of about 7.5, where both the xanthine residue and the phosphate group are deprotonated (see also Figure 1 and reference [34]).

textbooks. In Figure 4 also the discussed $(N1)^-/(N3)H$ and $(N1)H/(N3)^-$ tautomerism is indicated as is the partial delocalization of the negative charge on $(N)^-$ towards the (C)O groups.[34]

2.4 At which nitrogen site do metal ions coordinate to the xanthine residue? In a study[30] evaluating the binding modes in metal-ion complexes formed with xanthosine, deprotonation at (N3)H is favored, yet application of $\log K_{\text{complex stability}}$ versus pK_a straight-line plots for (N1)-type nitrogen ligands like inosine yields reasonable results. Indeed, with the conclusions of Section 2.3 in mind this is not too much of a surprise. Furthermore it is concluded[30] that in solution significant portions of the metal ions are N7-coordinated in their xanthosinate complexes. Indeed, X-ray diffraction analyses of $[M(xanthosinate)_2(H_2O)_4]\cdot 2H_2O$, in which $M^{2+}=Ni^{2+}$ (cf. reference [35]) or Zn^{2+} (cf. reference [36]), reveal N7 binding of the metal ions in the solid state, but they imply also that the (N3)H site is deprotonated, with $(N3)^-$ and (N1)H as well as the two (C)O groups being involved in a complicated hydrogen-bonding network.

The above contrasts with the solid-state structure of the already mentioned titanocene–xanthine 3:1 complex,[32] in which the N1 and N9 sites are deprotonated. In this molecule the Ti^{III} of $[Ti(\eta^5\text{-}C_5H_5)_2]^+$ forms a five-membered chelate with N7 and (C6)O as well as a four-membered chelate with $(N1)^-$ and (C2)O; the third $[Ti(\eta^5\text{-}C_5H_5)_2]^+$ interacts in a monodentate manner with $(N9)^-$ and a Cl^- ion. Most remarkable is that the (N3)H unit in this complex is still intact. All this indicates that a shift from a (N3)H to a (N1)H deprotonation is easily achieved in the xanthine residue.

Interesting in this connection is that methylation at N7 favors (N1)H deprotonation; i.e., the (N1)H-deprotonated tautomer reaches a higher formation degree in 7-methylxanthine compared with that in 9-methylxanthine.[7] Because metal ions like to bind in aqueous solution to N7 of neutral xanthosine[37] as well as in related hypoxanthine and guanine derivatives,[21,38–40] one expects that this binding mode due to the positive charge close to N7 favors (N1)H deprotonation[41] also in xanthine derivatives. Of course, the negative charge at $(N1)^-$ will partially be delocalized to the neighboring carbonyl groups (Figure 4). However, this delocalization does not necessarily lead to chelate formation of the N7-coordinated metal ion with the neighboring (C6)O group, though it is possible,[32] and in the form of seven-membered semichelates involving a water molecule bound to the metal ion and a hydrogen bond to (C6)O it is easily achieved, as is evident from the solid-state examples mentioned above.[35,36]

Hence, we conclude that N7–metal-ion binding of a xanthosinate residue appears to be the rule, whereas the site of deprotonation, (N1)H or (N3)H, in such complexes is more ambiguous. Tentatively we favor (N1)H deprotonation for aqueous solutions, because this should also facilitate outer-sphere binding to (C6)O. Indeed this conclusion is in accord with the results discussed in the sections to follow.

2.5 Stability constants of M^{2+} complexes formed with XMP: Because in $H_3(XMP)^+$ the first proton is mainly released from the $P(O)(OH)_2$ group and the second one from the $(N7)H^+$ unit (see the second to the last paragraph in Section 2.1), N7 becomes available for metal-ion binding in the $H(XMP)^-$ species, which may also be written as $(XMP{\cdot}H)^-$, because the proton is at the phosphate group. Consequently, the first complex to be considered has the composition $M(H;XMP)^+$. Naturally, the ligand species XMP^{2-} $(=(X-H{\cdot}MP{\cdot}H)^{2-}$; see Section 2.2) and $(XMP-H)^{3-}$ $(=(X-H{\cdot}MP)^{3-})$ may also form complexes with the divalent metal ions considered in this study and hence, the following three complex equilibria [Eqs. (8)–(10)] need to be taken into account:

$$M^{2+} + H(XMP)^- \rightleftharpoons M(H;XMP)^+ \quad (8a)$$

$$K^{M}_{M(H;XMP)} = [M(H;XMP)^+]/([M^{2+}][H(XMP)^-]) \quad (8b)$$

$$M^{2+} + XMP^{2-} \rightleftharpoons M(XMP) \quad (9a)$$

$$K^{M}_{M(XMP)} = [M(XMP)]/([M^{2+}][XMP^{2-}]) \quad (9b)$$

$$M^{2+} + (XMP-H)^{3-} \rightleftharpoons M(XMP-H)^{-} \quad (10a)$$

$$K^{M}_{M(XMP-H)} = [M(XMP-H)^{-}]/([M^{2+}][(XMP-H)^{3-}]) \quad (10b)$$

Considering that $pK^{H}_{H_2(XMP)} = 0.97 \pm 0.15$ (Section 2.1), it is immediately evident that the stability of the $M(H;XMP)^{+}$ complexes [Eq. (8)] cannot be measured via potentiometric pH titrations, the evaluation of which rests on the observation of a buffer depression in the presence of metal ions compared to the situation in their absence. Such a buffer depression at $pH < 1$ is too small to be reliably measured. Because metal ions bind to N7 in these complexes, it might be possible to determine their stability constants by means of UV spectrophotometric measurements, though the success of such experiments is rather questionable as the change in absorption upon metal ion coordination is expected to be small[42,43] and the protonation equilibria are overlapping as well as complicated (Section 2.1);[7] furthermore, the N7/H^{+} interactions will be reflected in the same wavelength range.[42,43] Therefore, the stability of the $M(H;XMP)^{+}$ complexes will be estimated in Section 2.6.

Because complex formation with the ligand species XMP^{2-} and $(XMP-H)^{3-}$ [Eqs. (9) and (10)] occurs in a pH range easily accessible for potentiometric pH titrations, this method was employed and all experiments aimed to determine stability constants of metal-ion complexes were carried out with an M^{2+} concentration in excess of the ligand (L) concentration. This means that under the experimental conditions (see Section 4.4) only 1:1 complexes form; indeed, there was no indication for the formation of either ML_2 or M_2L species.

In fact, the experimental data of the potentiometric pH titrations can be completely described by considering Equilibria (3), (4), (9), and (10), provided the evaluation is not carried into the pH range in which hydroxo complexes form. The occurrence of this last reaction was easily identified from titrations in the absence of ligand (Section 4.4). The results obtained from the potentiometric experiments regarding the stabilities of the M(XMP) [Eq. (9)] and $M(XMP-H)^{-}$ [Eq. (10)] complexes are collected in columns 3 and 4, respectively, in Table 1.[44]

2.6 Estimation of the stability of the $M(H;XMP)^{+}$ complexes: With the situation regarding the $M(H;XMP)^{+}$ complexes as summarized in Section 2.5 in mind, we decided to make sophisticated estimates of the stabilities of the $M(H;XMP)^{+}$ complexes [Eq. (8)] by applying the previously determined[42] $\log K^{M}_{M(Bz)}$ versus $pK^{H}_{H(Bz)}$ straight-line plots, in which Bz represents benzimidazole-type ligands. It needs to be recalled in this context that 1-methylbenzimidazole may also be addressed as 9-methyl-1,3-dideazapurine, thus reflecting the close structural relationship between benzimidazoles and purines,[45] and therefore, the structural conditions of N3 of a benzimidazole derivative reflect well those of N7 of a purine derivative. Furthermore, the steric influence of a carbonyl oxygen atom neighboring N7 is known to be very small (much smaller than of an amino group),[46] if it exists at all.[47] For example, for the Co^{2+} and Ni^{2+} complexes of cytidine (Cyd) it was recently proven that the carbonyl group neighboring N3 in the pyrimidine ring has no measurable effect on the stability of these $M(Cyd)^{2+}$ complexes.[46]

Therefore, the mentioned straight-line plots[42] may be used to calculate stability constants for complexes formed between M^{2+} and the neutral xanthosine residue of the phosphate-monoprotonated $(XMP\cdot H)^{-}$ ligand, by using the known[7] micro acidity constant, $pk^{XMP\cdot H}_{H\cdot XMP\cdot H} = 1.11 \pm 0.08$ (Section 2.1), which reflects the deprotonation reaction of the $(N7)H^{+}$ unit in $(H\cdot XMP\cdot H)^{\pm}$. In other words, the stability constants calculated in this way refer to "theoretical" $M(xanthosine)^{2+}$ complexes, that is, of a xanthosine ligand with the mentioned pk_a value. Hence, these constants need to be further corrected[48] for the charge effect which the $P(O)_2(OH)^{-}$ group in $(XMP\cdot H)^{-}$ $(=H(XMP)^{-})$ exerts on M^{2+} coordinated at the N7 site; this charge effect amounts to 0.40 ± 0.15 log units, as is known[49,50] from various other cases in which the distances between the positive and negative charges are of a comparable size.

The results of the above calculations for the stabilities of the various $M(H;XMP)^{+}$ complexes [Eq. (6)] are listed in column 2 of Table 1, together with the generously estimated error limits of ± 0.3 log units. It

Table 1. Logarithms of the stability constants of $M(H;XMP)^{+}$ [Eq. (8); estimates], M(XMP) [Eq. (9)] and $M(XMP-H)^{-}$ [Eq. (10)] complexes as determined by potentiometric pH titrations in aqueous solution, together with the negative logarithms of the acidity constants [Eqs. (13), (14)] of the $M(H;XMP)^{+}$ [Eq. (11)] and M(XMP) [Eq. (12)] complexes (25 °C; $I = 0.1$ M, $NaNO_3$).[a,b]

M^{2+}	$\log K^{M}_{M(H;XMP)}$[c]	$\log K^{M}_{M(XMP)}$	$\log K^{M}_{M(XMP-H)}$	$pK^{H}_{M(H;XMP)}$	$pK^{H}_{M(XMP)}$
Ba^{2+}	0.2 ± 0.3	1.00 ± 0.09	1.66 ± 0.08	4.5 ± 0.3	5.79 ± 0.12
Sr^{2+}	0.2 ± 0.3	1.02 ± 0.08	1.69 ± 0.07	4.5 ± 0.3	5.78 ± 0.11
Ca^{2+}	0.25 ± 0.3	1.14 ± 0.03	1.87 ± 0.05	4.4 ± 0.3	5.72 ± 0.06
Mg^{2+}	0.25 ± 0.3	1.16 ± 0.16	2.07 ± 0.04	4.4 ± 0.35	5.54 ± 0.17
Mn^{2+}	0.3 ± 0.3	1.82 ± 0.07	2.89 ± 0.09	3.8 ± 0.3	5.38 ± 0.12
Co^{2+}	1.1 ± 0.3	2.38 ± 0.04	3.62 ± 0.07	4.0 ± 0.3	5.21 ± 0.08
Ni^{2+}	1.5 ± 0.3	2.67 ± 0.08	4.06 ± 0.08	4.1 ± 0.3	5.06 ± 0.11
Cu^{2+}	1.8 ± 0.3	3.31 ± 0.04	4.69 ± 0.06	3.8 ± 0.3	5.07 ± 0.07
Zn^{2+}	0.7 ± 0.3	2.26 ± 0.04	3.51 ± 0.05	3.75 ± 0.3	5.20 ± 0.07
Cd^{2+}	1.1 ± 0.3	2.62 ± 0.04	3.95 ± 0.08	3.8 ± 0.3	5.12 ± 0.09

[a] The acidity constants[7] for $H_2(XMP)^{\pm}$ are $pK^{H}_{H_2(XMP)} = 0.97 \pm 0.15$ [Eq. (2)], $pK^{H}_{H(XMP)} = 5.30 \pm 0.02$ [Eq. (3)], and $pK^{H}_{XMP} = 6.45 \pm 0.02$ [Eq. (4)] (see Section 2.1); so-called practical, mixed, or Brønsted acidity constants are given (see ref. [44]).[7] [b] The error limits given (except those in column 2) are three times the standard error of the mean value (3σ) or the sum of the probable systematic errors, whichever is larger. The error limits of the derived data, in the present case for columns 5 and 6, were calculated according to the error propagation after Gauss. [c] Estimated values; see Section 2.6.

is comforting to note that the previously estimated stabilities, based on experiments,[37] for the Co^{2+}, Ni^{2+}, Cu^{2+}, and Cd^{2+} complexes of xanthosine, if corrected for the charge effect and the different basicities of N7 by 0.7 ± 0.2 log units,[51] give the log stability constants 1.2 ± 0.3, 1.4 ± 0.3, 1.5 ± 0.35, and 1.4 ± 0.25, respectively, and that these values are within the error limits identical with those listed in column 2 of Table 1. Moreover, the stability constants of all the corresponding $M(H;IMP)^+$ complexes[52] are also identical within the error limits with the values listed in Table 1 for the $M(H;XMP)^+$ species; this last observation is easily understandable because $pK^H_{H_2(IMP)}=1.30\pm0.10$, which mainly quantifies the release of the proton from $(N7)H^+$,[21] is rather close to $pk^{XMP\cdot H}_{H\cdot XMP\cdot H}=1.11\pm0.08$ (Section 2.1).[53]

2.7 Preliminary evaluation of the stability and structure of the various XMP–metal-ion complexes: From a careful consideration of the equilibria discussed so far it is evident that the complex M(XMP) is not only formed according to Equilibrium (9), but also according to the following deprotonation reaction [Eq. (11)]:

$$M(H;XMP)^+ \rightleftharpoons M(XMP) + H^+ \quad (11a)$$

$$K^H_{M(H;XMP)} = [M(XMP)][H^+]/[M(H;XMP)^+] \quad (11b)$$

Similarly, the species $M(XMP-H)^-$ may not only originate from Equilibrium (10), but it may also form according to Equilibrium (12):

$$M(XMP) \rightleftharpoons M(XMP-H)^- + H^+ \quad (12a)$$

$$K^H_{M(XMP)} = [M(XMP-H)^-][H^+]/[M(XMP)] \quad (12b)$$

However, the acidity constants defined in Equations (11) and (12) are connected with the other equilibrium constants already mentioned in Sections 2.1 and 2.5 by the following Equations (13) and (14):

$$pK^H_{M(H;XMP)} = pK^H_{H(XMP)} + \log K^M_{M(H;XMP)} - \log K^M_{M(XMP)} \quad (13)$$

$$pK^H_{M(XMP)} = pK^H_{XMP} + \log K^M_{M(XMP)} - \log K^M_{M(XMP-H)} \quad (14)$$

The acidity constants calculated in this way for Equilibria (11) and (12) are listed in columns 5 and 6, respectively, of Table 1.

In Section 2.6 we have already seen that in the $M(H;XMP)^+$ complexes [Eq. (8) and Table 1, column 2] the metal ion is coordinated at the N7 site of the xanthosine residue, the proton being located at the phosphate group; therefore these species are best written as $(M\cdot XMP\cdot H)^+$ to reflect their structure. Of course, one expects that this binding mode facilitates deprotonation of the xanthine residue, probably largely at (N1)H (see Section 2.4), and indeed, the acidification according to Equation (15) (Section 2.1 and Table 1) varies for the different metal ions between about 0.8 to 1.5, being least pronounced for the alkaline earth ions and most pronounced for Cu^{2+}, Zn^{2+}, and Cd^{2+} as expected.

$$\Delta pK_{a/X} = pK^H_{H(XMP)} - pK^H_{M(H;XMP)} \quad (15)$$

The resulting complex species M(XMP) are best written as $(M\cdot X-H\cdot MP\cdot H)^\pm$ to reflect their structure, that is, the metal ion is at the xanthosinate residue with an overall charge of $+1$ and the proton is bound at the $P(O)_2(OH)^-$ group.

The stability constants of the metal-ion complexes formed with xanthosinate, $(Xao-H)^-$, are listed in the second column[37] of Table 2.[54] A comparison of the stability constants of these $M(Xao-H)^+$ complexes with those of the $(M\cdot X-H\cdot MP\cdot H)^\pm$ species (Table 1, column 3) reveals that the latter are more stable by about 0.6 to 1.0 log units. This stability enhancement is higher than expected[48] based on a simple charge effect of the $P(O)_2(OH)^-$ group; in fact, it indicates that to a certain extent macrochelates form between the N7-coordinated metal ions and the $P(O)_2(OH)^-$ residue (Figure 1). Such an observation involving a $P(O)_2(OH)^-$ group has been made before;[55] the extent of this macrochelate formation will be considered in Section 2.9.

Table 2. Logarithms of the stability constants[a] of the 1:1 complexes formed by M^{2+} with xanthosinate, $(Xao-H)^-$,[b] or with D-ribose 5-monophosphate, $RibMP^{2-}$,[c] in aqueous solution at 25 °C and $I=0.1$ M ($NaNO_3$).

M^{2+}	$\log K^M_{M(Xao-H)}$	$\log K^M_{M(RibMP)}$
Ba^{2+}	0.2 ± 0.2[d]	1.17 ± 0.03
Sr^{2+}	0.2 ± 0.2[d]	1.25 ± 0.02
Ca^{2+}	0.2 ± 0.2[d]	1.48 ± 0.01
Mg^{2+}	0.2 ± 0.2[d]	1.58 ± 0.02
Mn^{2+}	0.84 ± 0.05	2.20 ± 0.02
Co^{2+}	1.65 ± 0.05	2.00 ± 0.01
Ni^{2+}	2.09 ± 0.05	2.00 ± 0.01
Cu^{2+}	2.58 ± 0.03	2.96 ± 0.02
Zn^{2+}	1.32 ± 0.02	2.20 ± 0.02
Cd^{2+}	1.96 ± 0.05	2.49 ± 0.02

[a] For the error limits see footnote [b] of Table 1. [b] From reference [37]; $pK^H_{Xao}=5.47\pm0.03$. [c] From reference [54]; $pK^H_{H(RibMP)}=6.24.\pm0.01$. [d] These stability constants and their error limits are estimates.[37]

Of course, macrochelate formation as indicated in the preceding paragraph for the $(M\cdot X-H\cdot MP\cdot H)^\pm$ species [= M(XMP)] will facilitate deprotonation of the $P(O)_2(OH)^-$ group; this acidification as defined by Equation (16) (Section 2.1 and Table 1) amounts to about 0.7 to 1.4 pK units and it leads to the $M(XMP-H)^-$ complex species [Eq. (12); Table 1, column 6].

$$\Delta pK_{a/P} = pK^H_{XMP} - pK^H_{M(XMP)} \quad (16)$$

However, it is most revealing to consider in this context the stabilities of the complexes formed between metal ions and xanthosinate[37] on the one hand and ribose 5-monophosphate ($RibMP^{2-}$)[54] on the other. The corresponding

log stability constants are listed in columns 2 and 3, respectively, of Table 2.

Comparisons in Table 2 reveal 1) that the stability of M(RibMP) complexes is in most instances higher than the one of the $M(Xao-H)^+$ species; this then means that the metal ion in $(M{\cdot}X-H{\cdot}MP{\cdot}H)^{\pm}$ switches upon deprotonation of the $P(O)_2(OH)^-$ group from the N7 site to the phosphate groups in the $M(XMP-H)^-$ complexes. Furthermore, 2) the log stability constants of the $M(XMP-H)^-$ complexes (Table 1, column 4) are by about 0.4 to 2.1 log units larger than those of the M(RibMP) complexes (Table 2, column 3); this in part, despite the charge effect, dramatic stability enhancement can only mean that the phosphate-coordinated metal ion interacts in addition with N7 (none of the other N atoms is sterically accessible)[21] forming macrochelates. Of course, there must be an intramolecular equilibrium between "open" and "closed" (macrochelated) $M(XMP-H)^-$ species, and these are best designated as $(X-H{\cdot}MP{\cdot}M)^-_{op}$ and $(X-H{\cdot}MP{\cdot}M)^-_{cl}$; the position of this indicated intramolecular equilibrium will be evaluated in Sections 2.10 and 2.11.

2.8 Quantitative evaluation of the stability enhancement for the M(XMP) complexes: In the preceding section we have seen that the M(XMP) complexes [Eq. (9); Table 1, column 3] are best written as $(M{\cdot}X-H{\cdot}MP{\cdot}H)^{\pm}$ to reflect the fact that the metal ion is coordinated at N7 and that the proton is part of the $P(O)_2(OH)^-$ group. We have further seen that these complexes show an enhanced stability that is to be attributed to macrochelate formation of the N7-bound metal ion with the $P(O)_2(OH)^-$ residue. Hence, we now aim to quantify this stability enhancement, because once known it allows us to calculate the extent of chelate formation;[56] in other words, to determine the position of Equilibrium (17) between the open (op) and chelated or closed (cl) isomers:

$$(M\cdot X-H\cdot MP\cdot H)^{\pm}_{op} \rightleftharpoons (M\cdot X-H\cdot MP\cdot H)^{\pm}_{cl} \quad (17)$$

The stability enhancement is in the present case expressed by the stability difference $\log \Delta_{M/XMP}$, which is defined by Equation (18), in which $K^M_{M(XMP)}$ refers to Equation (9) (Table 1, column 3) and $K^M_{M(XMP)op}$ defines the stability of the open isomer [Eq. (19)]:

$$\log \Delta_{M/XMP} = \log K^M_{M(XMP)} - \log K^M_{M(XMP)op} \quad (18)$$

$$K^M_{M(XMP)op} = [(M\cdot X-H\cdot MP\cdot H)^{\pm}_{op}]/([M^{2+}][XMP^{2-}]) \quad (19)$$

From Equation (18) it is evident that it has to be the aim to obtain values for $K^M_{M(XMP)op}$. This goal is best achieved by correcting the known[37] stability constants of the $M(Xao-H)^+$ complexes (Table 2, column 2) for the difference in the basicities of the xanthine residue in the $(Xao-H)^-$ and $(X-H{\cdot}MP{\cdot}H)^{2-}$ species, as well as for the charge effect that the $P(O)_2(OH)^-$ group exercises on a metal ion coordinated at N7.

The mentioned basicity difference is defined by Equation (20):

$$\Delta pK_a = pk^{X-H\cdot MP\cdot H}_{XMP\cdot H} \text{ (see Section 2.2)} - pK^H_{Xao} \text{ (ref. [37])} \quad (20a)$$

$$= (5.35 \pm 0.02) - (5.47 \pm 0.03) \quad (20b)$$

$$= -0.12 \pm 0.04 \quad (20c)$$

At first sight it may seem surprising that the acidity of the species which carries the larger negative charge due to the presence of the $P(O)_2(OH)^-$ group is slightly higher ($\Delta pK_a = -0.12$). The reason is most likely that a hydrogen bond between the proton of the $P(O)_2(OH)^-$ group and N7 exists, leading to an acidification of the Xao residue. In fact, for several related examples the extent of such a hydrogen-bond formation in aqueous solution has been quantified recently.[57] The mentioned ΔpK_a value is now used to calculate, in conjunction with the slopes (m) of the $\log K^M_{M(Bz)}$ versus $pK^H_{H(Bz)}$ straight-line plots[42] of benzimidazole-type ligands (see also Section 2.6), the slightly reduced complex stability, which results from the reduced basicity; it may be mentioned that the slopes for other N-type systems[58,59] are very similar. The results of these calculations are listed in column 3 of Table 3 ($\log K^M_{M(Xao-H)cor}$). Comparison of the basicity-corrected values with those for the $M(Xao-H)^+$ complexes given in column 2 of Table 2 shows that the corrections are of a very minor order; this is not surprising because $\Delta pK_a = -0.12$ and $m < 0.4$ in all instances.

Table 3. Stability-constant comparisons[a] for the M(XMP) complexes between the measured stability constants ($K^M_{M(XMP)}$),[b] which encompass all isomers of Equilibrium (17), and the estimated ones for the open $(M{\cdot}X-H{\cdot}MP{\cdot}H)^{\pm}_{op}$ isomers ($K^M_{M(XMP)op}$),[c] which are based on the basicity-corrected stabilities of the M(xanthosinate)$^+$ complexes (column 3)[d] and which are then further corrected for the charge effect of the $P(O)_2(OH)^-$ group[c] to give the values listed in column 4 (aqueous solution; 25 °C; I = 0.1 M, $NaNO_3$).

M^{2+}	$\log K^M_{M(XMP)}$ [Eq. (9)][b]	$\log K^M_{M(Xao-H)cor}$ cf.[d]	$\log K^M_{M(XMP)op}$ [Eq. (19)][c]	$\log \Delta_{M/XMP}$ [Eq. (18)]
Ba^{2+}	1.00 ± 0.09	0.2 ± 0.2	0.6 ± 0.25	0.40 ± 0.27
Sr^{2+}	1.02 ± 0.08	0.2 ± 0.2	0.6 ± 0.25	0.42 ± 0.26
Ca^{2+}	1.14 ± 0.03	0.2 ± 0.2	0.6 ± 0.25	0.54 ± 0.25
Mg^{2+}	1.16 ± 0.16	0.2 ± 0.2	0.6 ± 0.25	0.56 ± 0.30
Mn^{2+}	1.82 ± 0.07	0.82 ± 0.05	1.22 ± 0.16	0.60 ± 0.17
Co^{2+}	2.38 ± 0.04	1.63 ± 0.05	2.03 ± 0.16	0.35 ± 0.16
Ni^{2+}	2.67 ± 0.08	2.07 ± 0.05	2.47 ± 0.16	0.20 ± 0.18
Cu^{2+}	3.31 ± 0.04	2.53 ± 0.03	2.93 ± 0.15	0.38 ± 0.16
Zn^{2+}	2.26 ± 0.04	1.29 ± 0.02	1.69 ± 0.15	0.57 ± 0.16
Cd^{2+}	2.62 ± 0.04	1.92 ± 0.05	2.32 ± 0.16	0.30 ± 0.16

[a] For the error limits see footnote [b] of Table 1. [b] These values are from column 3 of Table 1. [c] See text in Section 2.8. [d] These values are the constants of column 2 in Table 2 corrected for the different basicities of the xanthine residue in the $(Xao-H)^-$ and $(X-H{\cdot}MP{\cdot}H)^{2-}$ species.

The charge effect of the $P(O)_2(OH)^-$ residue on a metal ion at N7 amounts to 0.4 ± 0.15 log units as discussed in Section 2.6. Addition of this value to those listed in column 3 of

Table 3 gives the log stability constants, $\log K^{M}_{M(XMP)op}$, for the open $(M{\cdot}X{-}H{\cdot}MP{\cdot}H)^{\pm}_{op}$ isomer in Equilibrium (17); these constants appear in column 4 of Table 3.

Now we are in the position to calculate the $\log \Delta_{M/XMP}$ values according to Equation (18); these results vary between about 0.2 and 0.6 log units and they are listed in column 5 of Table 3. There are two interesting observations: 1) Despite the large error limits it is evident that the value for the Ni^{2+}system, $\log \Delta_{Ni/XMP} = 0.20$, is very small compared with the others listed in this column; this result confirms the usual observation that Ni^{2+} has a notoriously low affinity toward phosphate groups, especially if compared with that of Mn^{2+}.[21,60,61] 2) All the other $\log \Delta_{M/XMP}$ values are very similar; in fact, they are within the error limits identical with the average of the remaining nine values (i.e., ignoring the one for Ni^{2+}), which equals $0.46 \pm 0.11 (3\sigma)$ log units. This similarity indicates[55] that the interaction of the N7-coordinated metal ions with the $P(O)_2(OH)^-$ group occurs largely in an outer-sphere manner; and this of course leads also to similar formation degrees of the macrochelated species (see below).

2.9 Extent of macrochelate formation involving the $P(O)_2(OH)^-$ group in the $(M{\cdot}X{-}H{\cdot}MP{\cdot}H)^{\pm}$ species: Following previous routes,[18,56,61] the application of the $\log \Delta_{M/XMP}$ values [Eq. (18); Table 3, column 5] allows to define the position of the intramolecular Equilibrium (17); that is, to calculate values for the dimensionless equilibrium constant, $K^{*}_{I/H}$, according to Equation (21):

$$K^{*}_{I/H} = \frac{[(M \cdot X{-}H \cdot MP \cdot H)^{\pm}_{cl}]}{[(M \cdot X{-}H \cdot MP \cdot H)^{\pm}_{op}]} \quad (21a)$$

$$= \frac{K^{M}_{M(XMP)}}{K^{M}_{M(XMP)op}} - 1 \quad (21b)$$

$$= 10^{\log \Delta_{M/XMP}} - 1 \quad (21c)$$

Once $K^{*}_{I/H}$ is known, the formation degree or the percentage of the macrochelated or closed species in Equilibrium (17) follows then from Equation (22):

$$\%\,(M \cdot X{-}H \cdot MP \cdot H)^{\pm}_{cl} = 100\, K^{*}_{I/H}/(1 + K^{*}_{I/H}) \quad (22)$$

These formation degrees are listed in column 4 of Table 4.

In accord with the above discussion in Section 2.8 regarding the size of the $\log \Delta_{M/XMP}$ values it is no surprise that the formation degrees of the closed species (Table 4, column 4) vary only slightly and that all of them are, within the error limits, identical with the average formation degree of $64 \pm 9\%\,(3\sigma)$, neglecting again the Ni^{2+} system. However, it needs to be emphasized that the high formation degree of the macrochelates is a matter of the position of the concentration-independent intramolecular Equilibrium (17) and therefore it has little to do with the absolute stabilities of these complexes, which vary in fact quite significantly as is evident from the stability constants listed for the M(XMP) $[=(M{\cdot}X{-}H{\cdot}MP{\cdot}H)^{\pm}]$ complexes in the second column of Table 3.

Table 4. Extent of chelate formation in M(XMP) complexes [Eq. (17)] as calculated from the stability enhancement $\log \Delta_{M/XMP}$ [Eq. (18)] and quantified by the dimensionless equilibrium constant $K^{*}_{I/H}$ [Eq. (21)] and the percentage of the macrochelated isomers $(M{\cdot}X{-}H{\cdot}MP{\cdot}H)^{\pm}_{cl}$ [Eq. (22)] in aqueous solution (25 °C; $I = 0.1$ M, $NaNO_3$).[a]

M^{2+}	$\log \Delta_{M/XMP}$	$K^{*}_{I/H}$	% $(M{\cdot}X{-}H{\cdot}MP{\cdot}H)^{\pm}_{cl}$
Ba^{2+}	0.40 ± 0.27	1.51 ± 1.56	60 ± 25
Sr^{2+}	0.42 ± 0.26	1.63 ± 1.57	62 ± 23
Ca^{2+}	0.54 ± 0.25	2.47 ± 2.00	71 ± 17
Mg^{2+}	0.56 ± 0.30	2.63 ± 2.51	72 ± 19
Mn^{2+}	0.60 ± 0.17	2.98 ± 1.56	75 ± 10
Co^{2+}	0.35 ± 0.16	1.24 ± 0.82	55 ± 16
Ni^{2+}	0.20 ± 0.18	0.58 ± 0.66	37 ± 26
Cu^{2+}	0.38 ± 0.16	1.40 ± 0.88	58 ± 15
Zn^{2+}	0.57 ± 0.16	2.72 ± 1.37	73 ± 10
Cd^{2+}	0.30 ± 0.16	1.00 ± 0.74	50 ± 18

[a] For the error limits see footnote [b] of Table 1. The values in the second column are from the final column in Table 3.

However, the presented results regarding macrochelate formation are in accord with the conclusions summarized in Section 2.4 that the main binding site for metal ions at the xanthosine residue is N7, because in the *anti* conformation of XMP (Figure 1) only a metal ion coordinated to this N site is able to interact simultaneously with the monoprotonated phosphate residue. Maybe, here is a further reason for the low formation degree of $(Ni{\cdot}X{-}H{\cdot}MP{\cdot}H)^{\pm}_{cl}$, aside from the comparably low affinity of Ni^{2+} for phosphate residues (see Section 2.8), that is, that this metal ion coordinates partly at the $(N1)^-$ [or $(N3)^-$] site[30] and the $P(O)_2(OH)^-$ group is then not reachable.

It should be added that a 5′-phosphate group and N3 are simultaneously not accessible for metal ions for steric reasons, and for an N1/phosphate combination a transformation of the purine nucleotide into the *syn* conformation would be necessary, yet this *anti/syn* barrier[46] is with about 6–7.5 kJ mol^{-1} too large to be overcome by macrochelate formation. Of course, as pointed out already in Section 2.4 metal ion binding at N7 is expected to facilitate especially the deprotonation of the (N1)H site; it is therefore likely that in the $(M{\cdot}X{-}H{\cdot}MP{\cdot}H)^{\pm}$ species this proton was lost, though a tautomeric complex with a deprotonated (N3)H site occurring in equilibrium cannot be excluded.

2.10 Proof of an enhanced stability for several $M(XMP{-}H)^-$ complexes: In Section 2.7 we have seen that the metal ion in $(M{\cdot}X{-}H{\cdot}MP{\cdot}H)^{\pm}$ switches upon deprotonation of the $P(O)_2(OH)^-$ residue from the N7 site to the twofold negatively charged phosphate group and that this site becomes the stability determining site for the $M(XMP{-}H)^-$ complexes, which we may also write as $(X{-}H{\cdot}MP{\cdot}M)^-$, thus indicating that the xanthosine residue is deprotonated and the metal ion placed at the PO_3^{2-} group. It is therefore justified to apply the previously determined $\log K^{M}_{M(R\text{-}PO_3)}$ versus $pK^{H}_{H(R\text{-}PO_3)}$ plots for simple phosphate

monoesters[54] and phosphonates;[50] these ligands are abbreviated as R-PO_3^{2-}, where R represents a noninteracting residue. For families of related ligands such plots lead to straight lines,[56] which are defined in Equation (23) for the complexes of R-PO_3^{2-} species:[50]

$$\log K^{M}_{M(R\text{-}PO_3)} = m \cdot pK^{H}_{H(R\text{-}PO_3)} + b \qquad (23)$$

The parameters of Equation (23), that is, the slopes m and the intercepts b with the y axis have been determined[50] and tabulated.[21,50,61]

Two such plots are shown in Figure 5 for the Ca^{2+} and Cd^{2+} systems, as examples. Whereas the data point for the $Ca^{2+}/(XMP-H)^{3-}$ system is only about 0.4 log units above its reference line, a result possibly due only to a charge effect (see below), the point for the $Cd^{2+}/(XMP-H)^{3-}$ system is about 1.5 log units above its reference line and therefore definite proof for an enhanced complex stability, because this increase is far beyond any possible charge influence. In other words, this example proves that the following intramolecular Equilibrium (24) must exist at least for some

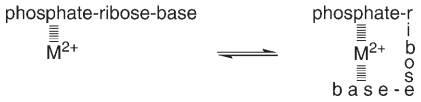

(24)

$M(XMP-H)^{-}$ complexes [Eq. (10); Table 1, column 4].

The parameters of the mentioned straight-line plots for $M(R\text{-}PO_3)$ complexes allow the calculation of the stability of the open isomer in Equilibrium (24) for a M^{2+} complex of an R-PO_3^{2-} ligand, in which the monoprotonated phosphate group has the intrinsic pk_a value discussed in Section 2.2; that is, $pk^{X-H\cdot MP}_{X-H\cdot MP\cdot H} = 6.40 \pm 0.04$ (Figure 2), and which refers to the deprotonation of the $(X-H\cdot MP\cdot H)^{2-}$ tautomer. With these calculated stabilities for "theoretical" $M(R\text{-}PO_3)$ complexes one may define the following stability difference:

$$\log \Delta_{M/R\text{-}PO_3} = \log K^{M}_{M(XMP-H)} - \log K^{M}_{M(R\text{-}PO_3)} \qquad (25)$$

The stability constants which appear in Equation (25) are listed in columns 2 and 3, respectively, of Table 5 and the values for $\log \Delta_{M/R\text{-}PO_3}$ are given in column 4. Since the complexes $M(XMP-H)^{-}$ and $M(R\text{-}PO_3)$, to which the listed

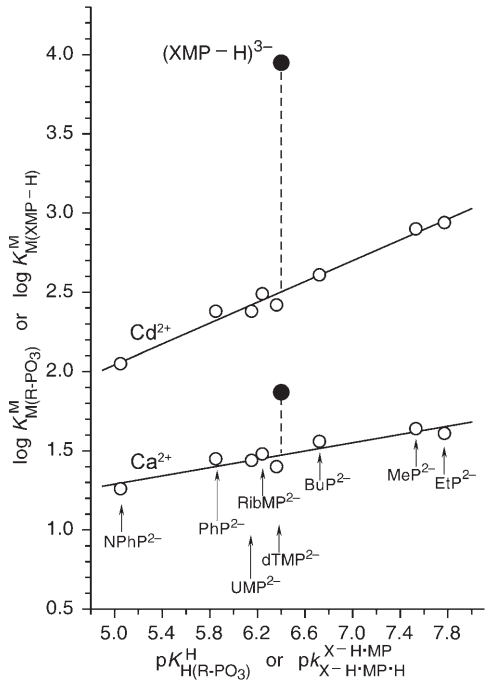

Figure 5. Evidence for an enhanced stability of the Ca^{2+} and Cd^{2+} (●) 1:1 complexes of $(XMP-H)^{3-}$ based on the relationship between $\log K^{M}_{M(R\text{-}PO_3)}$ and $pK^{H}_{H(R\text{-}PO_3)}$ for the 1:1 complexes of Ca^{2+} and Cd^{2+} with some simple phosphate monoester and phosphonate ligands (R-PO_3^{2-}; ○): 4-nitrophenyl phosphate ($NPhP^{2-}$), phenyl phosphate (PhP^{2-}), uridine 5′-monophosphate (UMP^{2-}), D-ribose 5-monophosphate ($RibMP^{2-}$), thymidine (=2′-deoxyribosylthymine) 5′-monophosphate ($dTMP^{2-}$), butyl phosphate (BuP^{2-}), methanephosphonate (MeP^{2-}), and ethanephosphonate (EtP^{2-}) (from left to right). The least-squares straight-reference lines are drawn through the corresponding eight data sets, which are taken for the phosphate monoesters from reference [54] and for the phosphonates from reference [50]; the parameters for these reference lines according to Equation (23) are listed in Table 5 of reference [50].[21,61] The points due to the equilibrium constants for the $M^{2+}/(XMP-H)^{3-}$ systems (●) are given in Table 1 and the micro acidity constant used, $pk^{X-H\cdot MP}_{X-H\cdot MP\cdot H} = 6.40 \pm 0.04$ is from Section 2.2 (Figure 2). All the plotted equilibrium constants refer to aqueous solutions at 25 °C and $I = 0.1$ M ($NaNO_3$). The vertical broken lines emphasize the stability differences to the corresponding reference lines; these differences equal $\log \Delta_{M/R\text{-}PO_3}$ as defined in Section 2.10 by Equation (25) and the corresponding values are listed in column 4 of Table 5.

Table 5. Stability-constant comparisons[a] for the $M(XMP-H)^{-}$ complexes between the measured stability constants ($K^{M}_{M(XMP-H)}$),[b] which encompass all isomers given in Equilibrium (24), and the calculated stability constants ($K^{M}_{M(R\text{-}PO_3)}$), which are based on the intrinsic basicity of the phosphate group[c] of $(XMP-H)^{3-}$ and the reference-line equations [Eq. (23)][c] and thus quantify the stabilities of the open, "theoretical" $M(R\text{-}PO_3)$ isomers in Equilibrium (24). The resulting stability differences, $\log \Delta_{M/R\text{-}PO_3}$, need to be corrected for the charge effect of the uncoordinated xanthosinate residue giving then the stability enhancement, $\log \Delta_{M/(XMP-H)}$, solely due to macrochelate formation according to Equilibrium (24) (aqueous solution; 25 °C; $I = 0.1$ M, $NaNO_3$).[a]

M^{2+}	$\log K^{M}_{M(XMP-H)}$ [Eq. (10)][b]	$\log K^{M}_{M(R\text{-}PO_3)}$[c]	$\log \Delta_{M/R\text{-}PO_3}$ [Eq. (25)]	$\log \Delta_{M/(XMP-H)}$ [Eq. (26)]
Ba^{2+}	1.66 ± 0.08	1.18 ± 0.04	0.48 ± 0.09	0.08 ± 0.17
Sr^{2+}	1.69 ± 0.07	1.26 ± 0.04	0.43 ± 0.08	0.03 ± 0.17
Ca^{2+}	1.87 ± 0.05	1.47 ± 0.05	0.40 ± 0.07	0.00 ± 0.17
Mg^{2+}	2.07 ± 0.04	1.60 ± 0.04	0.47 ± 0.06	0.07 ± 0.16
Mn^{2+}	2.89 ± 0.09	2.21 ± 0.05	0.68 ± 0.10	0.28 ± 0.18
Co^{2+}	3.62 ± 0.07	1.98 ± 0.06	1.64 ± 0.09	1.24 ± 0.17
Ni^{2+}	4.06 ± 0.08	1.99 ± 0.05	2.07 ± 0.09	1.67 ± 0.17
Cu^{2+}	4.69 ± 0.06	2.96 ± 0.06	1.73 ± 0.08	1.33 ± 0.17
Zn^{2+}	3.51 ± 0.05	2.19 ± 0.06	1.32 ± 0.08	0.92 ± 0.17
Cd^{2+}	3.95 ± 0.08	2.50 ± 0.05	1.45 ± 0.09	1.05 ± 0.17

[a] For the error limits see footnote [b] of Table 1. [b] These values are from column 4 of Table 1. [c] Calculated with the micro acidity constant $pk^{X-H\cdot MP}_{X-H\cdot MP\cdot H} = 6.40 \pm 0.04$ (Section 2.2) and the straight-line parameters[21,50,61] of Equation (23); see text in Section 2.10.

constants in columns 2 and 3, respectively, refer, differ by a charge of −1, there is a charge effect that the deprotonated xanthosine residue exerts on M^{2+} bound at the phosphate residue without any direct interaction. We need to take this effect into account and reduce the $\log \Delta_{M/R\text{-}PO_3}$ values correspondingly. As discussed in Section 2.6, this −/2+ charge effect amounts to 0.40 ± 0.15 log units; hence, we obtain from Equation (26) the $\log \Delta_{M/(XMP-H)}$ values that now solely quantify the enhanced stability due to macrochelate formation. These stability differences are listed in column 5 of Table 5.

$$\log \Delta_{M/(XMP-H)} = \log \Delta_{M/R\text{-}PO_3} - (0.40 \pm 0.15) \quad (26)$$

There are several observations that warrant recognition: 1) The stability enhancements for the complexes of the alkaline earth ions are small, if they exist at all; in other words, the affinity of these ions for N7 is insignificant, which is in agreement with experience.[59,62] 2) All 3d metal ions, as well as Zn^{2+} and Cd^{2+}, show an enhanced stability and thus, an affinity of the phosphate-bound metal ions towards N7; as indicated before (Section 2.9), another N site of the xanthine residue is sterically not accessible by a phosphate-coordinated metal ion in the *anti* conformation of XMP. 3) The affinity of Ni^{2+} toward N7 is most pronounced and this observation agrees with that made at other complexes of purine–nucleoside 5′-monophosphates.[21] This result has been explained[63] by considerations on the statistical effects in the context of the preferred coordination number of these metal ions, especially of $Ni^{2+}$and Cu^{2+}, and these effects favor Ni^{2+}.

2.11 Extent of macrochelate formation in the M(XMP−H)$^-$ complexes: If the open isomers in Equilibrium (24) are defined as $(X{-}H{\cdot}MP{\cdot}M)^-_{op}$ and the macrochelated or closed ones as $(X{-}H{\cdot}MP{\cdot}M)^-_{cl}$, the corresponding equilibrium constant K_I is defined by Equation (27) and values for K_I may be calculated[56] by Equation (28), which is defined in analogy to Equation (21c):

$$K_I = [(X{-}H \cdot MP \cdot M)^-_{cl}]/[(X{-}H \cdot MP \cdot M)^-_{op}] \quad (27)$$

$$K_I = 10^{\log \Delta_{M/(XMP-H)}} - 1 \quad (28)$$

Now Equation (28) can be applied and the intramolecular equilibrium constants K_I [Eq. (27)] can be obtained and in analogy to Equation (22) the formation degrees of the macrochelates indicated in Equilibrium (24) can be calculated. These results are summarized in Table 6.

Of course, due to the large error limits that are due to the estimation of the charge effect, the extent of macrochelate formation in the $(X{-}H{\cdot}MP{\cdot}M)^-$ species of the alkaline earth ions is not well defined (Table 6, column 4); however, it is still certain that it is smaller than in the case of the protonated $(M{\cdot}X{-}H{\cdot}MP{\cdot}H)^{\pm}$ species (Table 4, column 4). A possible reason could be that the alkaline earth ions bound to N7 (possibly in an outer-sphere manner) in the phosphate-protonated species are very flexible and can therefore easily reach the monoprotonated phosphate group. This is most likely different in the $(X{-}H{\cdot}MP{\cdot}M)^-$ complexes, because alkaline earth ions tend to bind in a semichelate-type fashion to a PO_3^{2-} group, that is, one oxygen atom of the phosphate group is inner-sphere and another one outer-sphere coordinated;[54] in this way much of the flexibility would be lost and thus, the interaction, even in an outer-sphere manner, with N7 reduced. In any case, for the M(IMP) and M(GMP) complexes a low degree of chelate formation with the alkaline earth ions was observed,[21] and therefore the present result is in line with these earlier observations.

Table 6. Extent of chelate formation in M(XMP−H)$^-$ complexes [Eq. (24)] as calculated from the stability enhancement $\log \Delta_{M/(XMP-H)}$ [Eq. (26)] and quantified by the dimensionless equilibrium constant K_I [Eqs. (27,28)] and the percentage of the macrochelated isomers $(X{-}H{\cdot}MP{\cdot}M)^-_{cl}$ [analogous to Eq. (22)] in aqueous solution (25 °C; I = 0.1 M, $NaNO_3$).[a]

M^{2+}	$\log \Delta_{M/(XMP-H)}$	K_I	% $(X{-}H{\cdot}MP{\cdot}M)^-_{cl}$
Ba^{2+}	0.08 ± 0.17	0.202 ± 0.471	≈0 (17 ± 33)
Sr^{2+}	0.03 ± 0.17	0.072 ± 0.419	≈0 (7 ± 37)
Ca^{2+}	0.00 ± 0.17	0.000 ± 0.391	≈0 (0 ± 39)
Mg^{2+}	0.07 ± 0.16	0.175 ± 0.433	≈0 (15 ± 31)
Mn^{2+}	0.28 ± 0.18	0.905 ± 0.790	48 ± 22
Co^{2+}	1.24 ± 0.17	16.38 ± 6.80	94 ± 2
Ni^{2+}	1.67 ± 0.17	45.77 ± 18.31	98 ± 1
Cu^{2+}	1.33 ± 0.17	20.38 ± 8.37	95 ± 2
Zn^{2+}	0.92 ± 0.17	7.32 ± 3.26	88 ± 5
Cd^{2+}	1.05 ± 0.17	10.22 ± 4.39	91 ± 3

[a] For the error limits see footnote [b] of Table 1. The values in the second column are from the final column in Table 5.

For the $(X{-}H{\cdot}MP{\cdot}M)^-$ complexes of Co^{2+}, Ni^{2+}, Cu^{2+}, Zn^{2+}, and Cd^{2+}, macrochelate formation is high, that is, close to 90% or even higher. This is expected because the high affinity of these metal ions toward N sites is well known,[62] and the result is again in line with that obtained for the corresponding M(IMP) and M(GMP) complexes.[21] As far as macrochelate formation is concerned, the properties of the corresponding Mn^{2+} complexes are between those of the alkaline earth ions and those of Co^{2+}, Ni^{2+}, Cu^{2+}, Zn^{2+}, and Cd^{2+}; again, a result in line with general experience[62] in coordination chemistry.

2.12 A new view on the macrochelate effect and its quantification for the M(XMP−H)$^-$ complexes: The so-called "chelate effect" refers to the enhanced stability of a complex formed by a ligand offering two or more donor atoms,[64] thus giving rise to the formation of chelate rings. There have been several attempts to quantify the chelate effect (for details see reference [55]). A recently described method,[55] in which care was taken to make sure that numbers with the same dimension were compared (which unfortunately in the literature is very often *not* the case) was applied to six-membered chelates. The principal point for the application of this method is that the metal-ion affinity of the sites participating in chelate formation can be quantified in an inde-

Table 7. Quantification of the chelate effect according to Equation (31) for several $M(XMP-H)^-$ complexes based on the intrinsic metal ion affinity of the individual binding sites, that is, of the phosphate group ($\log k^M_{(PO_3\cdot M/XMP-H)}$) and the xanthosinate site ($\log k^M_{(Xao\cdot M/XMP-H)}$) [Eq. (29)] of $(XMP-H)^{3-}$. The values for $\log Chelate$ [column 9; Eq. (31)] are a measure for the chelate effect in the various $(XMP-H)^-$ species (aqueous solution; 25 °C; $I=0.1$ M, $NaNO_3$).[a]

M^{2+}	$\log K^M_{M(R\text{-}PO_3)}$[b]	$\log k^M_{(PO_3\cdot M/XMP-H)}$[c]	$\log K^M_{M(Xao-H)}$[d]	$\log K^M_{M(Xao-H)B,cor}$[c]	$\log k^M_{(Xao\cdot M/XMP-H)}$[c]	$\log K^M_{M(XMP-H)}$ measured[e]	expected[f]	$\log Chelate$[g]
Ba^{2+}	1.18±0.04	1.58±0.16	0.2±0.2	0.2±0.2	0.8±0.25	1.66±0.08	1.65±0.14	0.01±0.16
Sr^{2+}	1.26±0.04	1.66±0.16	0.2±0.2	0.2±0.2	0.8±0.25	1.69±0.07	1.72±0.14	−0.03±0.16
Ca^{2+}	1.47±0.05	1.87±0.16	0.2±0.2	0.2±0.2	0.8±0.25	1.87±0.05	1.91±0.15	−0.04±0.16
Mg^{2+}	1.60±0.04	2.00±0.16	0.2±0.2	0.2±0.2	0.8±0.25	2.07±0.04	2.03±0.15	0.04±0.16
Mn^{2+}	2.21±0.05	2.61±0.16	0.84±0.05	0.85±0.05	1.45±0.16	2.89±0.09	2.64±0.15	0.25±0.17
Co^{2+}	1.98±0.06	2.38±0.16	1.65±0.05	1.66±0.05	2.26±0.16	3.62±0.07	2.63±0.11	0.99±0.13
Ni^{2+}	1.99±0.05	2.39±0.16	2.09±0.05	2.10±0.05	2.70±0.16	4.06±0.08	2.87±0.12	1.19±0.14
Cu^{2+}	2.96±0.06	3.36±0.16	2.58±0.03	2.60±0.03	3.20±0.15	4.69±0.06	3.59±0.11	1.10±0.13
Zn^{2+}	2.19±0.06	2.59±0.16	1.32±0.02	1.33±0.02	1.93±0.15	3.51±0.05	2.68±0.13	0.83±0.14
Cd^{2+}	2.50±0.05	2.90±0.16	1.96±0.05	1.97±0.05	2.57±0.16	3.95±0.08	3.07±0.12	0.88±0.14

[a] For the error limits see footnote [b] of Table 1. [b] From column 3 in Table 5. [c] See text in Section 2.12. [d] From column 2 of Table 2. [e] From column 4 of Table 1. [f] Calculated according to Equation (29b). [g] Calculated according to Equation (31).

pendent manner and then an "expected" stability can be calculated. This method is now applied for the first time to the formation of macrochelates.

For the ligand $(XMP-H)^{3-}$ (Figure 4), which is central to this study, it has been shown in Section 2.11 that its $M(XMP-H)^-$ ($=(X-H\cdot MP\cdot M)^-$) complexes exist to a certain extent in the form of macrochelates [Eq. (24); Table 6]. Furthermore, for this ligand the rare opportunity exists to quantify the metal-ion affinity of the xanthosinate site (Section 2.8) and the PO_3^{2-} group (Section 2.10) individually. The sum of these two intrinsic micro stability constants, which has the dimension M^{-1} like the experimentally measured constant [Eq. (10)], provides the expected metal-ion affinity of the two individual binding sites in $(XMP-H)^{3-}$ [Eq. (29)]:

$$K^M_{M(XMP-H)expected} = \frac{[(PO_3\cdot M/XMP-H)^-] + [(Xao\cdot M/XMP-H)^-]}{[M^{2+}][(XMP-H)^{3-}]} \quad (29a)$$

$$= k^M_{(PO_3\cdot M/XMP-H)} + k^M_{(Xao\cdot M/XMP-H)} \quad (29b)$$

Values for the first micro stability constant of Equation (29b) can be calculated by applying the micro acidity constant, $pk^{X-H\cdot MP}_{X-H\cdot MP\cdot H}=6.40\pm0.04$ (Section 2.2), to Equation (23); these values have already been calculated (Table 5, column 3) and they are listed again in the second column of Table 7. These stability constants need to be corrected for the charge effect that the uncoordinated but negatively charged xanthosinate residue exercises on a metal ion bound to the PO_3^{2-} group. This effect amounts to 0.40± 0.15 log units (Section 2.6); hence, this value needs to be added to the constants listed in column 2 to give the micro stability constants for the $(PO_3\cdot M/XMP-H)^-$ species formed at the phosphate site of $(XMP-H)^{3-}$ (Table 7, column 3).

Values for the second micro stability constant in Equation (29b) are obtained by employing the known[37] stability constants of the xanthosinate complexes, $M(Xao-H)^+$. These values are provided in column 4 of Table 7 and they need to be corrected for the difference in basicity of the xanthine residue in xanthosinate and in $(XMP-H)^{3-}$. This difference is expressed in Equation (30):

$$pk^{X-H\cdot MP}_{XMP} - pK^H_{Xao} = (5.52\pm0.04;\ \text{Section 2.2}) - (5.47\pm0.03;\ \text{ref. [37]}) = 0.05\pm0.05 \quad (30)$$

Application of the slopes of the $\log K^M_{M(Bz)}$ versus $pK^H_{H(Bz)}$ straight-line plots (Sections 2.6 and 2.8) leads to the basicity-corrected $K^M_{M(Xao-H)B,cor}$ values listed in column 5. It is evident from Table 7 that these corrections are very minor. More important is the effect that the uncomplexed, twofold negatively charged PO_3^{2-} group has on metal ion (M^{2+}) binding at the xanthosinate residue; this charge effect amounts to 0.60±0.15 log units[65–68] and may be compared with the 0.40±0.15 log units due to the singly charged $P(O)_2(OH)^-$ group (Sections 2.6 and 2.10). Addition of 0.60 log units to the values in column 5 gives the logarithms of the micro stability constants $\log k^M_{(Xao\cdot M/XMP-H)}$ listed in column 6; they quantify the metal-ion affinity of the xanthosinate residue in the $(XMP-H)^{3-}$ ligand.

Now the expected stability of $M(XMP-H)^+$ complexes can be calculated according to Equation (29b); these values are listed in column 8 of Table 7. In other words, now the expected stability constants, $\log K^M_{M(XMP-H)expected}$ [Eq. (29a)], for $M(XMP-H)^-$ complexes without chelate formation but based on the M^{2+} affinity of the two binding sites are known, and therefore we can define the chelate effect[55] according to Equation (31) by comparing the expected stability constant with the one actually measured [Eq. (10)]:[69]

$$\log Chelate = \log K^M_{M(XMP-H)} - \log K^M_{M(XMP-H)expected} \quad (31)$$

The values for the three terms which appear in Equation (31) are listed in columns 9, 7, and 8, respectively, in Table 7.

Comparison of the log *Chelate* values in column 9 of Table 7 reveals that the chelate effect differs dramatically for the various $M(XMP-H)^-$ complexes. For the alkaline earth ions the effect is zero within the error limits in accord with the results seen in column 4 of Table 6, whereas for $Ni(XMP-H)^-$ it amounts to about 1.2 log units, indicating a significant macrochelate effect. Of course, the observed chelate effect parallels the formation degrees of the macrochelates as discussed in Section 2.11, the values of which are listed in column 4 of Table 6.

Because the ΔH^0 values, which reflect the binding strength between M^{2+} and a ligating site, are not expected to vary much for a given metal–ligand bond, be it in a monodentate or a chelated species, one may conclude in accord with earlier suggestions that the chelate effect is mainly an entropy effect,[70] though bond distortion in a chelate may affect ΔH^0 as well.[71] Clearly, for a detailed answer calorimetric measurements would be needed for each system to reveal the exact ΔH and ΔS contributions.

2.13 Formation degrees of the $M(XMP-H)^-$ isomers based on the definition of the macrochelate effect: Because the definition of the macrochelate effect as given in Equation (31) is based on the micro stability constants of the individual metal-ion binding sites [Eq. (29)], knowledge of log *Chelate* should allow not only the calculation of the formation degree of the macrochelate, but also of the species in which M^{2+} is solely bound either to the phosphate group or to the xanthosinate residue of $(XMP-H)^{3-}$. Evidently, this knowledge is of relevance for biological systems because it demonstrates how metal ions can switch from one site to another through macrochelate formation.

At this point it is helpful to investigate the implications of Equation (31) a bit more in detail.[55] From this equation follows Equation (32):

$$10^{\log Chelate} = K^{M}_{M(XMP-H)}/K^{M}_{M(XMP-H)expected} \quad (32a)$$

$$= K^{M}_{M(XMP-H)}/(k^{M}_{(PO_3\cdot M/XMP-H)} + k^{M}_{(Xao\cdot M/XMP-H)}) \quad (32b)$$

$$= \frac{[M(XMP-H)^-]}{[M^{2+}][(XMP-H)^{3-}]} \times \frac{[M^{2+}][(XMP-H)^{3-}]}{[(PO_3\cdot M/XMP-H)^-] + [(Xao\cdot M/XMP-H)^-]} \quad (32c)$$

$$= \frac{[M(XMP-H)^-]}{[(PO_3\cdot M/XMP-H)^-] + [(Xao\cdot M/XMP-H)^-]} \quad (32d)$$

According to this definition [Eq. (32)] $10^{\log Chelate}$ is the dimensionless equilibrium constant that quantifies the position of Equilibrium (33):

$$((PO_3\cdot M/XMP-H)^- + (Xao\cdot M/XMP-H)^-) \rightleftharpoons M(XMP-H)^- \quad (33)$$

In this equilibrium the left side contains the sum of the "open" species resulting from metal-ion binding to the individual sites of $(XMP-H)^{3-}$, whereas $M(XMP-H)^-$ at the right hand side represents the *total* amount of complexes formed including the chelates. The meaning of this dimensionless expression [Eq. (32d)] is further clarified below.

For $\log Chelate = 0$ in Equation (31), the ratio given in Equation (32d) equals one; this means, as it should be, that no chelates exist and that all $M(XMP-H)^-$ species are present as monodentatally coordinated $(PO_3\cdot M/XMP-H)^-$ and $(Xao\cdot M/XMP-H)^-$ complexes.

For all situations in which $\log Chelate > 0$, the ratio will be larger than 1 and this then means that chelated $M(XMP-H)^-$ species exist. For example, for $\log Chelate = 0.3$ a value of 2:1 follows for the ratio [Eq. (34)]:

$$\frac{[M(XMP-H)^-]}{[(PO_3\cdot M/XMP-H)^-] + [(Xao\cdot M/XMP-H)^-]} = \frac{2}{1} = \frac{1+1}{1} \quad (34)$$

This means, 50% of all $M(XMP-H)^-$ complexes exist in the form of chelates (it should be remembered here [see Eq. (10)] that $[M(XMP-H)^-]$ encompasses all complex species present). In the case that $\log Chelate = 1$ the ratio equals 10:1 giving Equation (35) and showing thus that 90% of the $M(XMP-H)^-$ species are present in the form of chelates.

$$\frac{[M(XMP-H)^-]}{[(PO_3\cdot M/XMP-H)^-] + [(Xao\cdot M/XMP-H)^-]} = \frac{10}{1} = \frac{9+1}{1} \quad (35)$$

In other words, Equations (31) and (32) represent a method to quantify the chelate effect by putting the formation degree of the chelated species in relation to that of their monodentate complexes.

Of course, the two monodentatally bound species, $(PO_3\cdot M/XMP-H)^-$ and $(Xao\cdot M/XMP-H)^-$, are also in equilibrium with each other. The position of this equilibrium is defined by the ratio of the two micro stability constants given in Equation (29b), the values of which are listed in columns 3 and 6 of Table 7. Application of this information allows one to calculate the formation degrees of all the species present in a $M(XMP-H)^-$ system, that is, the amount of "closed" or macrochelated $M(XMP-H)^-_{cl}$ species present (the calculations not being based on the definition of a primary binding site as in Sections 2.10 and 2.11) and consequently, also of the total amount of "open" species, $M(XMP-H)^-_{op/tot}$; application of the micro stability constants to these percentages gives then those of the open $(PO_3\cdot M/XMP-H)^-$ and $(Xao\cdot M/XMP-H)^-$ complexes. The corresponding results are listed in Table 8 and a tentative structure of the $M(XMP-H)^-$ macrochelate is shown in Figure 6.

There are several important conclusions possible from these results: First of all, it is satisfying to see that the formation degrees of the chelated species $M(XMP-H)^-_{cl}$ in Table 8 (column 3) are very similar and actually overlap within the error limits with the results given in Table 6

Table 8. Summary of the formation degrees of the chelated species, $M(XMP-H)^{-}_{cl}$, of the total open species, $M(XMP-H)^{-}_{op/tot}$, as well as of the open phosphate- and xanthosinate-coordinated complexes, $(PO_3{\cdot}M/XMP-H)^{-}$ and $(Xao{\cdot}M/XMP-H)^{-}$, as calculated [Eq. (32)] based on the extent of the chelate effect [Eq. (31)] and the micro stability constants for individual binding of the metal ions (Table 7) either to the phosphate group or the xanthosinate residue [Eq. (29)] (aqueous solution; 25 °C; $I = 0.1$ M, $NaNO_3$).[a]

M^{2+}	log *Chelate*[b]	% $M(XMP-H)^{-}_{cl}$[c]	% $M(XMP-H)^{-}_{op/tot}$[c]	% $(PO_3{\cdot}M/XMP-H)^{-}$[d]	% $(Xao{\cdot}M/XMP-H)^{-}$[d]
Ba^{2+}	0.01 ± 0.16	≈ 0	≈ 100[e]	86	14
Sr^{2+}	-0.03 ± 0.16	≈ 0	≈ 100[e]	88	12
Ca^{2+}	-0.04 ± 0.16	≈ 0	≈ 100[e]	92	8
Mg^{2+}	0.04 ± 0.16	≈ 0	≈ 100[e]	94	6
Mn^{2+}	0.25 ± 0.17	43.8 ± 22.0	56.2 ± 22.0	52.6	3.6
Co^{2+}	0.99 ± 0.13	89.8 ± 3.1	10.2 ± 3.1	5.8	4.4
Ni^{2+}	1.19 ± 0.14	93.5 ± 2.1	6.5 ± 2.1	2.1	4.4
Cu^{2+}	1.10 ± 0.13	92.1 ± 2.4	7.9 ± 2.4	4.7	3.2
Zn^{2+}	0.83 ± 0.14	85.2 ± 4.8	14.8 ± 4.8	12.1	2.7
Cd^{2+}	0.88 ± 0.14	86.8 ± 4.2	13.2 ± 4.2	9.0	4.2

[a] For the error limits see footnote [b] of Table 1. [b] From column 9 in Table 7. [c] The percentage of $M(XMP-H)^{-}_{op/tot}$ follows from Equation (32d) because the total amount of $M(XMP-H)^{-}$ complex present equals 100 %; hence, it follows further that $\%\, M(XMP-H)^{-}_{cl} = 100 - \%\, M(XMP-H)^{-}_{op/tot}$. [d] Application of the micro stability constants of the $(PO_3{\cdot}M/XMP-H)^{-}$ and $(Xao{\cdot}M/XMP-H)^{-}$ species to the total amount of $M(XMP-H)^{-}_{op/tot}$ present, allows calculation of the percentages of the monodentatally bound isomers (see also text in Section 2.13). The listed values are only estimations due to the large error limits of the micro stability constants (see Table 7, columns 3 and 6), but these values prove that both open isomers exist in equilibrium. [e] Because for the complexes of the alkaline earth ions log *Chelate* is zero within the error limits we assumed in the above calculations that only the open complexes occur but of course the $M(XMP-H)^{-}_{cl}$ species may still be formed in low amounts.

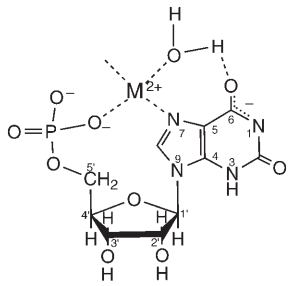

Figure 6. Tentative and simplified structure of $M(XMP-H)^{-}$ macrochelates. The extent of the hydrogen bond to the (C6)O group of a metal-ion-coordinated water molecule will certainly vary significantly from metal ion to metal ion as may be concluded from other related cases;[19,21] this means that possibly also the charge distribution towards (C2)O varies.

(column 4) for $(X-H{\cdot}MP{\cdot}M)^{-}_{cl}$; these data from Table 6 have been calculated on the assumption that the PO_3^{2-} group acts as the primary binding site in chelate formation. The agreement confirms the internal reliability of all the constants employed including the various assumptions that had to be made. The only "significant" deviation between the results in Tables 6 and 8 occurs with $Ni(XMP-H)^{-}$; this is understandable because the assumption that the PO_3^{2-} group is the primary binding site is in this case only poorly fulfilled. The xanthosinate residue has a comparable or even slightly larger affinity for Ni^{2+} (see Table 2), as is also confirmed by the percentages for $(PO_3{\cdot}Ni/XMP-H)^{-}$ and $(Xao{\cdot}Ni/XMP-H)^{-}$ given in columns 5 and 6, respectively, of Table 8. Yet, at the same time the results for Ni^{2+} are also comforting because the formation degrees of 98 ± 1 % (Table 6) and 93.5 ± 2.1 % (Table 8) for the chelated species are not far apart from each other.

Finally, it should be emphasized that the evaluation procedure taking the chelate effect (log *Chelate*) into account together with the micro stability constants provides interesting insights into the equilibria involving the open species. These are clearly also of biological interest as, for example, the data for the $Mg(XMP-H)^{-}$ system demonstrate, in which the $(PO_3{\cdot}Mg/XMP-H)^{-}$ complex dominates with about 94 % (see Table 8). Similarly, about 85 % of the $Zn(XMP-H)^{-}$ system occurs in the form of macrochelates and of the remaining 15 % of the open isomers, about 12 % exist as phosphate-bound species, $(PO_3{\cdot}Zn/XMP-H)^{-}$, and 3 % are present as xanthosinate-coordinated isomers, $(Xao{\cdot}Zn/XMP-H)^{-}$.

3. Conclusions

Xanthosinate 5′-monophosphate (Figures 1 and 4) is a fascinating but also quite complicated ligand. The reason for this is that the xanthine residue is deprotonated before the final proton of the phosphate group is lost; that is, the $(X-H{\cdot}MP{\cdot}H)^{2-}$ species transforms only with $pK_a = 6.45$ [or more exact with the micro acidity constant $pk^{X-H{\cdot}MP}_{X-H{\cdot}MP{\cdot}H} = 6.40$ (Figure 2)] into $(X-H{\cdot}MP)^{3-}$, commonly written as $(XMP-H)^{3-}$ (Sections 2.1 and 2.2). In other words, in the physiological pH range XMP is threefold negatively charged and differs such from its related nucleotides IMP^{2-} and GMP^{2-} (Figure 1) considerably. This has consequences,[7] as also pointed out by Shugar et al.,[15] for previous studies of "various enzyme systems and metabolic pathways" in which this fact was overlooked (like very recently also in reference [22]), "including, amongst others, xanthine oxidase, purine phosphoribosyltransferases, IMP dehydrogenases, purine nucleoside phosphorylases, nucleoside hydrolases, the enzymes involved in the biosynthesis of caffeine, the development of xanthine nucleotide-directed G proteins, the pharmacological properties of alkylxanthines".[15]

The indicated acid–base properties also have consequences for the metal-ion affinities of this nucleotide, because they lead to the formation of $(M{\cdot}X-H{\cdot}MP{\cdot}H)^{\pm}$ species, which have the metal ion at the xanthosinate residue (largely at N7) and the proton at the phosphate group.

Moreover, all these complex species exist to about 65% in the form of macrochelates, with the exception of the Ni^{2+} complex, which reaches a formation degree of about 35% only (Section 2.9, Table 4). This similarity in macrochelate formation indicates outer-sphere binding to the $P(O)_2(OH)^-$ group.

Furthermore, upon deprotonation of the phosphate group the metal ion switches in most instances from the deprotonated xanthine residue to the now twofold negatively charged phosphate group, because the latter binding site has in most cases the larger affinity for the metal ions considered. Of course, these $(X-H\cdot MP\cdot M)^-$ complexes may also form macrochelates (Section 2.11, Table 6) by an interaction of the phosphate-coordinated metal ion with N7 of the deprotonated xanthine residue. This deprotonation probably occurs mostly at (N1)H, but possibly to some extent also at (N3)H (see Sections 2.4 and 2.9). Surprisingly, in a first approximation it appears that the extent of macrochelate formation in $M(XMP-H)^-$ complexes (Table 6 and Table 8) is comparable to that[21] in M(IMP) and M(GMP) species. However, a more careful comparison reveals that the increased charge at the nucleobase residue leads indeed to a more pronounced stability enhancement [Eq. (26)] for the $M(XMP-H)^-$ complexes (Tables 5 and 6) relative to that[21] for the M(IMP) and M(GMP) species.

There is another point to be emphasized: The transfer from the $(M\cdot X-H\cdot MP\cdot H)^{\pm}$ to the $(X-H\cdot MP\cdot M)^-$ species occurs in aqueous solution with an average pK_a of about 5.5 (Table 1). However, it is known[72,73] that a decrease in the dielectric constant (ε; permittivity) of the solvent increases the pK_a considerably for the release of a proton from a phosphate group. For example, the change from water (ε ca. 80) to water containing 50% (v/v) 1,4-dioxane (ε ca. 35) increases such a pK_a value by more than 1 log unit;[73] that is, under such conditions $pK^H_{M(XMP)}$ increases to about 6.5 or more, close to the physiological pH range and at lower ε values this range will of course be reached. Since it is known[74,75] that in active-site cavities intrinsic dielectric constants of about 35 can easily be achieved,[75] the occurrence of these monoprotonated complexes in biological systems is quite likely and may thus affect the reactions[15] of XMP in enzymes and metabolic pathways.

No doubt, the coordination chemistry of XMP is very rich and varies from metal ion to metal ion. This is also fascinating with regard to the macrochelate effect, which could be quantified in this case by a recently developed new method[55] (Sections 2.12 and 2.13), because previously the individual metal-ion-binding properties of xanthosinate[37] and the phosphate group[21,61] had been characterized. These earlier achievements enabled us to obtain the intrinsic micro stability constants of the metal-ion complexes formed with the $(XMP-H)^{3-}$ ligand and to calculate not only the extent of macrochelate formation, but in addition the formation degrees of the various monodentate bound isomers. It is evident that the same method may also be applied to other macrochelates relevant in supramolecular chemistry or for biological systems.

4. Experimental Section

4.1 Materials: The disodium salt of xanthosine 5′-monophosphate was the same as used recently.[7] The disodium salt of 1,2-diaminoethane-*N*,*N*,*N*′,*N*′-tetraacetic acid (Na_2H_2EDTA), potassium hydrogen phthalate, HNO_3, NaOH (Titrisol), and the nitrate salts of Na^+, Mg^{2+}, Ca^{2+}, Sr^{2+}, Ba^{2+}, Mn^{2+}, Co^{2+}, Ni^{2+}, Cu^{2+}, Zn^{2+}, and Cd^{2+} (all pro analysi) were from Merck KGaA, Darmstadt (Germany). All solutions were prepared with deionized, ultrapure (MILLI-Q 185 PLUS, from Millipore S.A., 67120 Molsheim, France), and CO_2-free water.

The aqueous stock solution of XMP was freshly prepared daily, and its exact concentration was newly determined each time by titrations with NaOH (see below). The titer of the NaOH used for the titrations was established with potassium hydrogen phthalate. The exact concentrations of the stock solutions of the divalent metal ions were determined by potentiometric pH titrations via their EDTA complexes by measuring the equivalents of protons liberated from $H(EDTA)^{3-}$ upon complex formation.

4.2 Potentiometric pH titrations: The pH titrations were carried out with the Metrohm potentiograph used earlier[7] and the instrument was calibrated with buffers as described.[7] The direct pH-meter readings were used to calculate the acidity constants,[7] which are therefore so-called practical, mixed, or Brønsted constants.[44] Their negative logarithms (aqueous solution; 25 °C; $I=0.1$ M; $NaNO_3$) may be converted into the corresponding concentration constants[44] by subtracting 0.02 from the listed pK_a values (see also ref. [7]).

The ionic product of water (K_W) and the mentioned conversion term do not enter into our calculation procedures because we evaluate the *differences* in NaOH consumption between a pair of solutions; that is, a solution with and one without ligand are always titrated (see also below; for further details refs. [44] and [49] may be consulted). The stability constants for the metal-ion complexes are, as usual, concentration constants.

All equilibrium constants were calculated by curve-fitting procedures by using a Newton–Gauss nonlinear least-squares program in the way and with the computer equipment described recently.[33,76]

4.3 Determination of the acidity constants of $H(XMP)^-$: The acidity constants $K^H_{H(XMP)}$ [Eq. (3)] and K^H_{XMP} [Eq. (4)] were determined by titrating aqueous HNO_3 (50 mL, 0.54 mM; 25 °C; $I=0.1$ M; $NaNO_3$) in the presence and absence of XMP (0.3 mM; adjusted in its stock solutions to pH 5.9) under N_2 with NaOH (1.5 mL, 0.03 M). The experimental data were collected every 0.1 pH unit in the pH range 3.7–8.2 and used for the calculations; this range corresponds initially to about 2% neutralization for the equilibrium $H(XMP)^-/XMP^{2-}$ [Eq. (3)] and finally, to about 98% neutralization for the equilibrium $XMP^{2-}/(XMP-H)^{3-}$ [Eq. (4)].[7]

The results were the averages of 25 independent pairs of titrations for the acidity constants $K^H_{H(XMP)}$ [Eq. (3)] and K^H_{XMP} [Eq. (4)] as described in reference [7].

4.4 Determination of the stability constants of the M(XMP) and $M(XMP-H)^-$ complexes: The stability constants $K^M_{M(XMP)}$ [Eq. (9)] and $K^M_{M(XMP-H)}$ [Eq. (10)] were determined under the experimental conditions described above for the determination of the acidity constants $K^H_{H(XMP)}$ and K^H_{XMP}. However, $NaNO_3$ was partly or fully replaced by $M(NO_3)_2$ (25 °C; $I=0.1$ M). The M^{2+}/ligand ratios were 111:1 (Mg^{2+}, Ca^{2+}, Sr^{2+}, Ba^{2+}), 89:1 (Mg^{2+}, Ca^{2+}), 56:1 (Mn^{2+}, Co^{2+}, Ni^{2+}, Zn^{2+}, Cd^{2+}), 44:1 (Co^{2+}, Ni^{2+}), 28:1 (Mn^{2+}, Zn^{2+}, Cd^{2+}), 11:1 and 5.6:1 (Cu^{2+}). The stability constants $K^M_{M(XMP)}$ and $K^M_{M(XMP-H)}$ were calculated for each pair of titrations by taking into account the species H^+, $H(XMP)^-$, XMP^{2-}, $(XMP-H)^{3-}$, M^{2+}, M(XMP), and $M(XMP-H)^-$. The additional consideration of the $M(H;XMP)^+$ complex (see Section 2.5) in the calculations had within the error limits no effect on the results. The experimental data were collected every 0.1 pH unit from the lowest pH which could be reached in an experiment (at the most pH 3.2) to about 90% of deprotonated XMP^{2-}, that is, $(XMP-H)^{3-}$, or to the beginning of the hydrolysis of $M(aq)^{2+}$; the latter was evident from the titrations without ligand.

For all systems it holds that the results showed no dependence on the excess of M^{2+} used in the experiments. The final results given for the sta-

bility constants of the complexes are the averages of five independent pairs of titrations for each system.

Acknowledgement

The competent technical assistance of Astrid Sigel in the preparation of this manuscript and stimulating discussions with members of the COST D20 programme are gratefully acknowledged. This study was supported by the University of Basel and within the COST D20 programme by the Swiss State Secretariat for Education and Research.

[1] J. D. Rawn, *Biochemistry*, Patterson, Burlington, **1989**, pp. 636–639 and pp. 651–655.
[2] Y. Noguchi, N. Shimba, Y. Kawahara, E. Suzuki, S. Sugimoto, *Eur. J. Biochem.* **2003**, *270*, 2622–2626.
[3] R. B. Martin, Y. H. Mariam, *Met. Ions Biol. Syst.* **1979**, *8*, 57–124.
[4] a) R. Tribolet, H. Sigel, *Eur. J. Biochem.* **1987**, *163*, 353–363; b) N. A. Corfù, R. Tribolet, H. Sigel, *Eur. J. Biochem.* **1990**, *191*, 721–735.
[5] N. A. Corfù, H. Sigel, *Eur. J. Biochem.* **1991**, *199*, 659–669.
[6] K. Aoki, *Met. Ions Biol. Syst.* **1996**, *32*, 91–134.
[7] S. S. Massoud, N. A. Corfù, R. Griesser, H. Sigel, *Chem. Eur. J.* **2004**, *10*, 5129–5137.
[8] H. Sigel, *Pure Appl. Chem.* **2004**, *76*, 375–388.
[9] H. Sigel, *Chem. Soc. Rev.* **2004**, *33*, 191–200.
[10] H. R. Mahler, E. H. Cordes, *Biological Chemistry*, Harper & Row, New York, and John Weatherhill, Tokyo, **1966**, pp. 731–733.
[11] a) S. J. Lippard, J. M. Berg, *Bioanorganische Chemie* (translated by S. Müller-Becker), Spektrum, Heidelberg, **1995**, p. 341; b) R. Hille, *Met. Ions Biol. Syst.* **2002**, *39*, 187–226; c) D. J. Lowe, *Met. Ions Biol. Syst.* **2002**, *39*, 455–479.
[12] *IUPAC Stability Constants Database*, Release 5, Version 5.16 (compiled by L. D. Pettit, H. K. J. Powell), Academic Software, Timble, Otley, West Yorkshire (UK), **2001**.
[13] *NIST Critically Selected Stability Constants of Metal Complexes*, Reference Database 46, Version 6.0 (data collected and selected by R. M. Smith, A. E. Martell), US Department of Commerce, National Institute of Standards and Technology: Gaithersburg, MD (USA), **2001**.
[14] *Joint Expert Speciation System (JESS)*, Version 6.4 (joint venture by K. Murray, P. M. May), Division of Water Technology, CSIR, Pretoria (South Africa) and School of Mathematical and Physical Sciences, Murdoch University, Murdoch (Western Australia), **2001**.
[15] E. Kulikowska, B. Kierdaszuk, D. Shugar, *Acta Biochim. Pol.* **2004**, *51*, 493–531.
[16] R. K. O. Sigel, B. Song, H. Sigel, *J. Am. Chem. Soc.* **1997**, *119*, 744–755.
[17] H. Sigel, *Chem. Soc. Rev.* **1993**, *22*, 255–267.
[18] a) E. M. Bianchi, S. A. A. Sajadi, B. Song, H. Sigel, *Chem. Eur. J.* **2003**, *9*, 881–892; b) C. P. Da Costa, A. Okruszek, H. Sigel, *ChemBioChem* **2003**, *4*, 593–602.
[19] B. Knobloch, W. Linert, H. Sigel, *Proc. Natl. Acad. Sci. USA* **2005**, *102*, 7459–7464.
[20] H. Sigel, R. Griesser, *Chem. Soc. Rev.* **2005**, *34*, 875–900.
[21] a) H. Sigel, S. S. Massoud, N. A. Corfù, *J. Am. Chem. Soc.* **1994**, *116*, 2958–2971; b) H. Sigel, B. Song, *Met. Ions Biol. Syst.* **1996**, *32*, 135–205.
[22] Note added in proof: See, for example, R. A. Alberty, *Biophys. Chem.* **2006**, *121*, 157–162.
[23] a) K. H. Scheller, F. Hofstetter, P. R. Mitchell, B. Prijs, H. Sigel, *J. Am. Chem. Soc.* **1981**, *103*, 247–260; b) K. H. Scheller, H. Sigel, *J. Am. Chem. Soc.* **1983**, *105*, 5891–5900.
[24] O. Yamauchi, A. Odani, H. Masuda, H. Sigel, *Met. Ions Biol. Syst.* **1996**, *32*, 207–270.
[25] B. Lippert, *Prog. Inorg. Chem.* **2005**, *54*, 385–447.
[26] Maybe one should mention here for the expert or specialist that the values of the upper and lower circles, which constitute a microconstant Scheme (see, e.g., Figure 2), were deliberately estimated in ref. [7] independently of each other, instead of applying "known routes", because "the error limits of some of the acidity constants employed are rather large".[7] A consequence of this procedure is that a re-calculation of the macroconstants from the microconstants leads to somewhat different values; e.g., $K^{H}_{H_3(XMP)} = k^{XMP\cdot H_2}_{H\cdot XMP\cdot H_2} + k^{H\cdot XMP\cdot H}_{H\cdot XMP\cdot H_2} = 10^{-(0.71\pm0.37)} + 10^{-(0.3\pm0.2)}$ (see Figure 2 in [7]) $= 10^{-(0.16\pm0.18)}$. However, this re-calculated value, $pK^{H}_{H_3(XMP)} = 0.16 \pm 0.18$, for the macro acidity constant is within the error limits identical with the one given above in the text, that is, $pK^{H}_{H_3(XMP)} = 0.44 \pm 0.27$. It needs to be added that this latter value is in excellent agreement with other known acidity constants of $H_3(NMP)^+$ species (see Table 1 in reference [7]). Finally, for the micro acidity constant of the zwitterionic $(H\cdot XMP\cdot H)^{\pm}$ tautomer, $pk^{XMP\cdot H}_{H\cdot XMP\cdot H} = 1.11 \pm 0.08$, is certainly a reliable estimate (for details see reference [7] and also note [53] vide infra).
[27] J. R. Jones, S. E. Taylor, *J. Chem. Soc. Perkin Trans. 2* **1979**, 1253–1258.
[28] L. F. Cavalieri, J. J. Fox, A. Stone, N. Chang, *J. Am. Chem. Soc.* **1954**, *76*, 1119–1122.
[29] E. Buncel, B. K. Hunter, R. Kumar, A. R. Norris, *J. Inorg. Biochem.* **1984**, *20*, 171–181.
[30] R. B. Martin, *Met. Ions Biol. Syst.* **1996**, *32*, 61–89.
[31] H. Mizuno, T. Fujiwara, K. Tomita, *Bull. Chem. Soc. Jpn.* **1969**, *42*, 3099–3105.
[32] A. L. Beauchamp, F. Belanger-Gariepy, A. Mardhy, D. Cozak, *Inorg. Chim. Acta* **1986**, *124*, L23–L24.
[33] G. Kampf, L. E. Kapinos, R. Griesser, B. Lippert, H. Sigel, *J. Chem. Soc. Perkin Trans. 2* **2002**, 1320–1327.
[34] In the context of Figure 4 one is inclined to speculate that the $(N1)^-$ tautomer is even more important for $(X-H\cdot MP)^{3-}$ than it is for $(Xao-H)^-$, because for deprotonated 9-methylxanthine the $(N3)^-$ tautomer dominates strongly with about 95–99.9 %[7] meaning that the $(N1)^-$ tautomer occurs in very low concentration, whereas, as we have seen, for Xao it appears to be significant. It seems that the change in the ratio of the tautomers has to do with the solvation properties of the species; due to the sugar residue Xao is better solvated by water than 9MeXan. The presence of the phosphate group in XMP will further promote solvation and therefore we suspect that the concentration of the $(N1)^-$ tautomer will increase further. Indeed, the indicated hydrogen-bond formation (in Section 2.8) of $P(O)_2(OH)^-$ with N7 points into this direction. Furthermore, macrochelate formation or metal-ion binding at N7 is also expected to favor the $(N1)^-$ tautomer, because of outer-sphere hydrogen bonding to (C6)O; in addition, in the $(N1)^-$ tautomer the negative charge is also distributed over more atoms and here solvation comes in again. Of course, as said already in the text, it would be highly desirable that the various methylated derivatives of Xao and XMP are synthesized and their pK_a values measured, because this would allow an exact calculation of the concentration of the various tautomers.
[35] F. Barrios, J. M. Salas, M. P. Sánchez, M. Quirós, R. Faure, *J. Chem. Crystallogr.* **1999**, *29*, 1009–1013.
[36] M. Quirós, J. M. Salas, M. P. Sánchez, J. R. Alabart, R. Faure, *Inorg. Chem.* **1991**, *30*, 2916–2921.
[37] Y. Kinjo, R. Tribolet, N. A. Corfù, H. Sigel, *Inorg. Chem.* **1989**, *28*, 1480–1489.
[38] B. Song, J. Zhao, R. Griesser, C. Meiser, H. Sigel, B. Lippert, *Chem. Eur. J.* **1999**, *5*, 2374–2387.
[39] C. P. Da Costa, H. Sigel, *Inorg. Chem.* **2003**, *42*, 3475–3482.
[40] H. Sigel, *Pure Appl. Chem.* **2004**, *76*, 1869–1886.
[41] H. Sigel, *J. Am. Chem. Soc.* **1975**, *97*, 3209–3214.
[42] L. E. Kapinos, B. Song, H. Sigel, *Chem. Eur. J.* **1999**, *5*, 1794–1802.
[43] L. E. Kapinos, A. Holý, J. Günter, H. Sigel, *Inorg. Chem.* **2001**, *40*, 2500–2508.
[44] H. Sigel, A. D. Zuberbühler, O. Yamauchi, *Anal. Chim. Acta* **1991**, *255*, 63–72.

[45] a) J. C. Morales, E. T. Kool, *Nat. Struct. Biol.* **1998**, *5*, 950–954; b) K. M. Guckian, J. C. Morales, E. T. Kool, *J. Org. Chem.* **1998**, *63*, 9652–9656; c) J. C. Morales, E. T. Kool, *J. Am. Chem. Soc.* **1999**, *121*, 2323–2324.
[46] B. Knobloch, H. Sigel, *J. Biol. Inorg. Chem.* **2004**, *9*, 365–373.
[47] M. D. Reily, T. W. Hambley, L. G. Marzilli, *J. Am. Chem. Soc.* **1988**, *110*, 2999–3007.
[48] M. S. Lüth, L. E. Kapinos, B. Song, B. Lippert, H. Sigel, *J. Chem. Soc. Dalton Trans.* **1999**, 357–365.
[49] M. Bastian, H. Sigel, *J. Coord. Chem.* **1991**, *23*, 137–154.
[50] H. Sigel, D. Chen, N. A. Corfù, F. Gregáň, A. Holý, M. Strašák, *Helv. Chim. Acta* **1992**, *75*, 2634–2656.
[51] For the justification of this correction factor see ref. [21b], p. 162. It may be added that the given correction factor most likely also contains a contribution of macrochelate formation which is possible, for example, in $(Ni{\cdot}IMP{\cdot}H)^{+}$ but not in $Ni(inosine)^{2+}$; in fact, this situation corresponds to the one considered here.
[52] These constants are listed in a footnote to Table 9 on page 164 of ref. [21b].
[53] One could argue here that instead of $pK^{H}_{H_2(IMP)} = 1.30 \pm 0.10$, the micro acidity constant $pk^{IMP{\cdot}H}_{H{\cdot}IMP{\cdot}H} = 1.43 \pm 0.08$ (from ref. [21a]) should be compared with $pk^{XMP{\cdot}H}_{H{\cdot}XMP{\cdot}H} = 1.11 \pm 0.08$. However, because stability-constant evaluations of potentiometric pH titrations are based on macroconstants, we prefer the comparison given in the text. Moreover, for principal reasons it needs to be added that the slopes m of $\log K^{M}_{M(Bz)}$ versus $pK^{H}_{H(Bz)}$ straight line plots[42] are relatively small ($m < 0.4$) meaning that pK_a differences of the indicated kind have no effect within the given error limits on the listed log stability constants.
[54] S. S. Massoud, H. Sigel, *Inorg. Chem.* **1988**, *27*, 1447–1453.
[55] M. J. Sánchez-Moreno, A. Fernández-Botello, R. B. Gómez-Coca, R. Griesser, J. Ochocki, A. Kotynski, J. Niclós-Gutiérrez, V. Moreno, H. Sigel, *Inorg. Chem.* **2004**, *43*, 1311–1322.
[56] R. B. Martin, H. Sigel, *Comments Inorg. Chem.* **1988**, *6*, 285–314.
[57] a) H. Sigel, B. Lippert, *Pure Appl. Chem.* **1998**, *70*, 845–854; b) G. Kampf, M. S. Lüth, L. E. Kapinos, J. Müller, A. Holý, B. Lippert, H. Sigel, *Chem. Eur. J.* **2001**, *7*, 1899–1908; c) C. F. Moreno-Luque, E. Freisinger, B. Costisella, R. Griesser, J. Ochocki, B. Lippert, H. Sigel, *J. Chem. Soc. Perkin Trans. 2* **2001**, 2005–2011; d) M. J. Sánchez-Moreno, R. B. Gómez-Coca, A. Fernández-Botello, J. Ochocki, A. Kotynski, R. Griesser, H. Sigel, *Org. Biomol. Chem.* **2003**, *1*, 1819–1826.
[58] L. E. Kapinos, B. Song, H. Sigel, *Inorg. Chim. Acta* **1998**, *280*, 50–56.
[59] L. E. Kapinos, H. Sigel, *Inorg. Chim. Acta* **2002**, *337*, 131–142.
[60] a) A. Saha, N. Saha, L.-n. Ji, J. Zhao, F. Gregáň, S. A. A. Sajadi, B. Song, H. Sigel, *J. Biol. Inorg. Chem.* **1996**, *1*, 231–238; b) S. A. A. Sajadi, B. Song, F. Gregáň, H. Sigel, *Inorg. Chem.* **1999**, *38*, 439–448.
[61] H. Sigel, L. E. Kapinos, *Coord. Chem. Rev.* **2000**, *200–202*, 563–594.
[62] H. Sigel, D. B. McCormick, *Acc. Chem. Res.* **1970**, *3*, 201–208.
[63] H. Sigel, S. S. Massoud, R. Tribolet, *J. Am. Chem. Soc.* **1988**, *110*, 6857–6865.
[64] A. E. Martell, R. D. Hancock, R. J. Motekaitis, *Coord. Chem. Rev.* **1994**, *133*, 39–65.
[65] This value results from the inhibiting effect that a divalent metal ion (Pt^{2+}) at N7 of the adenine residue exercises on M^{2+} binding at the phosphonate group of $PMEA^{2-}$ [PMEA = 9-[2-(phosphonomethoxy)ethyl]adenine];[66] note, the distances between the charges in this nucleotide analogue[67] correspond to that in the present nucleotide. This earlier experimentally measured charge effect amounts to $0.59 \pm 0.05 (3\sigma)$ log units and it results from eight different metal-ion systems.[66] To be on the safe side, we extend the error limit considerably and use the value of 0.60 ± 0.15 log unit. It may be added that earlier for a similar situation the effect of a $-P(O)_2^{-}$-O-$P(O)_2(OH)^{-}$ group was estimated as 0.7 ± 0.2 log units (see footnote [44] of reference [60b] and footnote [2] of reference [68]).
[66] G. Kampf, M. S. Lüth, J. Müller, A. Holý, B. Lippert, H. Sigel, *Z. Naturforsch. B* **2000**, *55*, 1141–1152.
[67] a) C. A. Blindauer, A. Holý, H. Dvořáková, H. Sigel, *J. Chem. Soc. Perkin Trans. 2* **1997**, 2353–2363; b) C. H. Schwalbe, W. Thomson, S. Freeman, *J. Chem. Soc. Perkin Trans. 1* **1991**, 1348–1349.
[68] E. M. Bianchi, S. A. A. Sajadi, B. Song, H. Sigel, *Inorg. Chim. Acta* **2000**, *300–302*, 487–498.
[69] Due to discussions with colleagues we add that one might argue that in Equation (31) a statistical factor should be introduced, because once one of the monodentate ligands has coordinated to a metal ion then the second monodentate ligand finds a lower number of binding sites available at the metal ion. However, we prefer to ignore statistical effects for principle reasons (see below), though this would also be justified due to the smallness of the effect: The first coordinating ligand has six possibilities for binding at an octahedral coordinating sphere, whereas the second ligand has only five because one is already occupied; this statistical factor of 5/6 amounts to 0.08 log unit which should be deducted from the result obtained for the term at the right in Equation (29b) making $\log Chelate$ [Eq. (31)] a bit larger. Inspection of the results listed in column 9 of Table 7 shows that this effect is within the given error limits anyway. More importantly, we argue against the use of a statistical effect for principle reasons: Assuming that no chelate is formed but that both sites may bind a metal ion independently in a monodentate fashion, then the total (analytical) concentration of ML is simply given by the sum of the concentrations of the two individual isomers; clearly, statistics do not play a role here.
[70] a) N. Wiberg, *Holleman-Wiberg. Lehrbuch der Anorganischen Chemie*, Walter de Gruyter, Berlin, **1985**, p. 975; b) J. E. Huheey, *Anorganische Chemie. Prinzipien von Struktur und Reaktivität (translated from Inorganic Chemistry. Principles of Structure and Reactivity)* (Eds.: B. Reuter, B. Sarry), Walter de Gruyter, Berlin, **1988**, pp. 579–580.
[71] J. J. R. Fraústo da Silva, *J. Chem. Educ.* **1983**, *60*, 390–392.
[72] E. M. Bianchi, R. Griesser, H. Sigel, *Helv. Chim. Acta* **2005**, *88*, 406–425.
[73] G. Liang, N. A. Corfù, H. Sigel, *Z. Naturforsch. B* **1989**, *44*, 538–542.
[74] a) D. C. Rees, *J. Mol. Biol.* **1980**, *141*, 323–326; b) G. R. Moore, *FEBS Lett.* **1983**, *161*, 171–175; c) N. K. Rogers, G. R. Moore, M. J. E. Sternberg, *J. Mol. Biol.* **1985**, *182*, 613–616; d) G. Iversen, Y. I. Kharkats, J. Ulstrup, *Mol. Phys.* **1998**, *94*, 297–306.
[75] H. Sigel, R. B. Martin, R. Tribolet, U. K. Häring, R. Malini-Balakrishnan, *Eur. J. Biochem.* **1985**, *152*, 187–193. See also the comment in the footnote on page 258 in: M. Bastian, H. Sigel, *Inorg. Chim. Acta* **1990**, *178*, 249–259.
[76] a) C. A. Blindauer, T. I. Sjåstad, A. Holý, E. Sletten, H. Sigel, *J. Chem. Soc. Dalton Trans.* **1999**, 3661–3671; b) R. B. Gómez-Coca, L. E. Kapinos, A. Holý, R. A. Vilaplana, F. González-Vílchez, H. Sigel, *J. Chem. Soc. Dalton Trans.* **2000**, 2077–2084.

Received: February 4, 2006
Published online: August 3, 2006

